Investigation of Membrane Order within Integrin-Mediated Adhesion

by

Julia Tofalo Bourg

A dissertation submitted in partial fulfillment
of the requirements for the degree of
Doctor of Philosophy
(Biophysics)
in the University of Michigan
2018

Doctoral Committee

Associate Professor Sarah L. Veatch, Chair
Professor Myron K. Campbell
Assistant Professor Allen P. Liu
Professor Jennifer P. Ogilvie

“Although my publications contain meticulous details of plants that did grow, the runs that went smoothly, and the data that materialized, they perpetuate a disrespectful amnesia against the entire gardens that rotted in fungus and dismay ... I know damn well that if there had been a way to get to success without traveling through disaster someone would have done it and thus rendered the experiments unnecessary.”

- Hope Jahren

Julia T. Bourg

jtbourg@umich.edu

ORCID iD: 0000-0002-0214-0678

Dedication

This dissertation is dedicated to my parents, Anne and Jim. This exists because of and for, them.

Acknowledgements

I would like to thank my advisor, Sarah Veatch, who is a remarkable scholar and scientist, and helped shape this project and guide me through its twists and turns. Thank you to my committee members Jennifer Ogilvie, Myron Campbell, and Allen Liu for their guidance, support, and helpful discussions over the years. I want to express my sincere appreciation for the support that Jennifer and Myron gave me during my transition into Sarah's lab halfway through my graduate career, without them, it would not have been possible. I would also like to acknowledge Chris Meiners, Krishnan Raghunathan, and Joel Revalee for their support during the early years of my graduate career.

Thank you to my labmates, Marcos Núñez, Kathleen Wisser, Sarah Shelby, Brian DeVree, Matt Stone, and Thomas Shaw for sharing your expertise, patience, and comradery. I am so lucky that I got to work with such smart and talented people each day.

I would not be where I am today without my undergraduate mentors, Stan Tozer, Ewa Bienkiewicz, and Brad Groveman. Thank you to Stan for introducing me to the world of research. Thank you to Ewa and Brad, who helped instill a love for interdisciplinary science and did everything they could to make sure I would be able to pursue my graduate education in Biophysics. I have been incredibly lucky to have the support of many faculty and staff during my graduate career at Michigan; I would like to especially thank Christine Aidala, Naomi Mirkin, Cinda-Sue Davis, Jamie Saville, and Debbie Taylor who always made time to check in and give advice when I needed it.

I am deeply indebted to the members of the Michigan Society for Women in Physics (SWIP) who created a lasting support network throughout my graduate career (and beyond!). Thank you all my friends and colleagues, I would like to especially thank Jenna Walrath, Betsy Brown, Jenny Wong, Sam Pappas, Qi Zhang, Stephanie Miller, Veronica Policht, Renee Maenle, and Julia Eubanks. Without their friendship and support, graduate school would have been impossible. I cherish all of the fun times we had at Michigan together. Finally, thank you to my family, especially my parents, Anne and Jim, and my brother, Daniel.

Table of Contents

Lists of Abbreviations

ECM: Extracellular matrix
FAK: Focal Adhesion Kinase
EGF: Epidermal growth factor
VASP: Vasodilator-stimulated phosphoprotein
MIDAS: Metal ion-dependent adhesion site
ADMIDAS: Adjacent to Metal Ion Dependent Adhesion site
SyMBS: Synergistic metal ion binding site
PTB: Phosphotyrosine binding
FERM: four point one, ezrin radixin, moesin domain
MP: membrane-proximal
GPMVs: Giant Plasma Membrane Vesicles
Ld: Liquid-disordered phase
Lo: Liquid-ordered phase
αX: Where X is a number refers to a specific alpha subunit of a heterodimeric integrin pair
βX: Where X is a number refers to a specific beta subunit of a heterodimeric integrin pair
SMase: Sphingomyelinase
C8-LacCer: C8 – lactosylceraminde
GPI – AP: glycosylphosphatidylinositol-anchored proteins
NSOM: near-field scanning optical microscopy
STORM: Stochastic Optical Reconstruction Microscopy
dSTORM: direct Stochastic Optical Reconstruction Microscopy
PALM: Photo-activation localization microscopy
MEF: Mouse Embryonic Fibroblast
mEos3.2: Monomeric Eos photoactivable protein, clone 3.2
PM: a mEos3.2 photoactivatable fluorescent protein lipidated through saturated palmitoyl and myristoyl modifications from the 11 N-terminal residues of the Tyrosine-protein kinase, Lyn.
TM: mEos3.2 photoactivatable fluorescent protein-tagged attached to a short transmembrane peptide. The transmembrane sequence was derived from a 36-residue helix from the Linker -for-Activation-of-T-Cells
LAT: Linker for Activation of T-Cells
DBSCAN: Density-Based Spatial Clustering of Applications with Noise
RPMI: Roswell-Park Memorial Institute Medium
PBS: Phosphate Buffered Saline
IgG: Immunoglobulin G
TIRF: Total Internal Reflection Fluorescence
MAP: Mitogen Activation Protein
IRM: Interference Reflection Microscopy

DMEM: Dulbecco's Modified Eagle's Medium
HEPES: 4-(2-hydroxyethyl)-1-piperazineethanesulfonic acid
DMSO: Dimethyl sulfoxide
NHS: N-hydroxysuccinimide Ester
Src: Proto-oncogene tyrosine-protein kinase Src
FERM: Four point one (4.1) protein, Ezrin, radixin, moesin domain
PIPKIγ: Phosphatidylinositol phosphate kinase type Iγ
FAT: Focal adhesion targeting domain
SFK: Src Family Kinase
PIP2: phosphatidylinositol 4,5 bisphosphate (PIP2)
CAS: Cellular Apoptosis Susceptibility protein
Crk: Adaptor molecule crk or p38
Rac: Ras-related C3 botulinum toxin substrate, Subfamily of the Rho family of GTPases
RhoA: Ras homolog gene family, member A
PI-3K: Phosphatidylinositol-4,5-bisphosphate 3-kinase
Akt: Protein Kinase B, also known as PKB
MAPK: Mitogen-activated protein kinase
ERK: Extracellular signal-regulated kinases

List of Figures

List of Equations

Abstract

Integrins are transmembrane adhesion receptors that engage ligands in the extracellular matrix and cytoskeletal proteins to form multi-protein adhesive complexes. These complexes provide a platform for integrin signaling and a mechanical anchor between the cell and its environment. Integrin functionality is hypothesized to be sensitive to cell membrane composition, driven at least in part, by the tendency for the plasma membrane to compartmentalize into ordered and disordered domains resembling coexisting liquid phases observed in model membranes. In particular, past work suggests that adhesions are highly ordered membrane domains and that more integrins in an extended confirmation favor a more ordered membrane environment.

This dissertation investigates how integrins associate with membrane order through newly developed super-resolution imaging techniques that are capable of directly observing the local enrichment and depletion of peptide markers of liquid-ordered and disordered domains. I quantify the local membrane environment surrounding β1 integrins by tabulating cross-correlations between antibody labeled β1 integrins and peptide markers. Through the use of conformational specific antibodies, I determine how the conformational state of integrins impacts its local membrane composition and how membrane perturbations alter β1 integrin activity.

I find that β1 integrins co-localize with both markers of membrane order and disorder across the plasma membrane. I find that affinity for a membrane ordered probe depends on activation state and that β1 integrins from mature fibrillar adhesive complexes exhibit the strongest preference for membrane order. I determine that adhesions themselves are made up of integrins in

at least two different conformational states, and active, extended conformation integrins do not exhibit a strong preference for either phase-like domain composition despite being confined to adhesions. Finally, I demonstrate that perturbing the plasma membrane composition with long-chain *n*-alcohols robustly affects the activation state of β1 integrins and the formation of adhesive complexes.

The structure-function relationship of integrins has broad biological implications contributing to cell viability, growth, and motility. My work indicates that integrin association with membrane order is more subtle than previously proposed and that the subset of integrins in the active, extended conformation is less order preferring than the total integrin population. I show integrin activity is modulated by perturbations of membrane organization, and I conclude that integrin activation is indirectly impacted by membrane order, likely through the regulatory networks responsible for "inside-out" signaling.

Chapter 1: Introduction

The research detailed in this dissertation examines how the conformational state of integrins, a transmembrane adhesion receptor, dictates its local membrane environment and how membrane perturbations alter integrin activity. This chapter begins by introducing the components of integrin-mediated adhesion and reviews the current view on how integrins are activated. I also review the evidence that argues integrins and integrin containing adhesive complexes' function is sensitive to their local membrane composition. Finally, I introduce principles of super-resolution localization microscopy, the method used in this work to report on the spatial distribution of lipids surrounding integrins.

1.1 Integrin adhesion complexes: at the forefront of cell homeostasis and motility

1.1.1 Composition and formation of integrin-based adhesion complexes

Poised on the surface of the cell membrane are adhesion receptors that interpret a diverse set of environmental cues necessary to maintain proper cell growth, morphology, and viability[6, 7]. The principal class of cell-extracellular matrix (ECM) adhesions are those mediated by the integrin family, a set of receptors that connect the ECM to the actin cytoskeleton. The ECM is an extensive meshwork of insoluble proteins (e.g., collagen, fibronectin) and various proteoglycans that provide a stiff, yet flexible architecture, to which cells can adhere. Integrins are heterodimeric transmembrane protein complexes which integrate the extracellular and intracellular spaces [8]. On the cytosolic side, integrin tails bind to numerous protein binding partners that mediate signals or provide scaffolding to the actin cytoskeleton; these interactions are known collectively as the

"Integrin Adhesome" [9, 10]. These proteins fall into three categories: structural/scaffolding (e.g., talin, vinculin), enzymatic (e.g., focal adhesion kinase (FAK), Rho GTPases), and adaptor (e.g., paxillin, zyxin).

Adhesive complexes or contacts form when integrins bind to their various intra- and extracellular partners, and subsequently cluster to form dense multi-protein complexes (Figure 1-1).

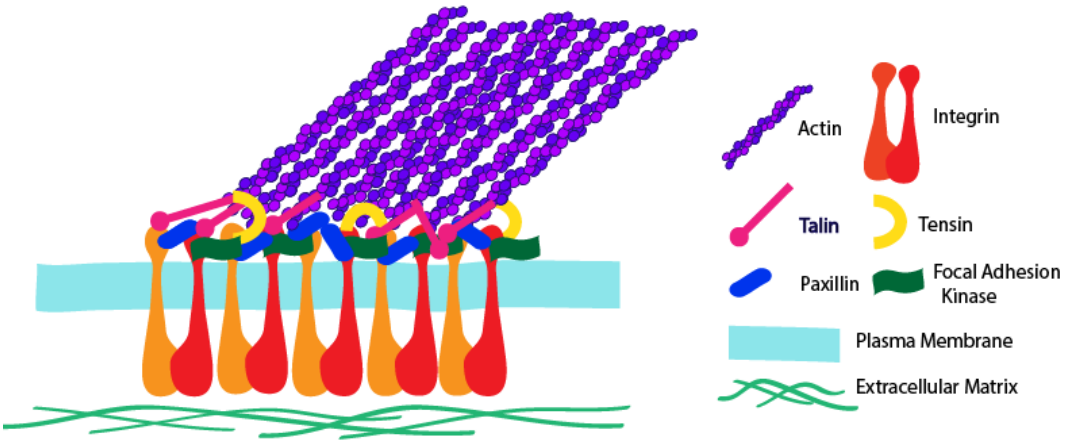

Figure 1-1: Components of integrin adhesion complexes

Integrins are heterodimeric transmembrane protein complexes which integrate the intra- and extracellular spaces (orange and red). By partnering with ligands in the extracellular matrix and numerous intracellular partners, they cluster to form dense protein complexes known as adhesion complexes or focal adhesions. Figure modified from [5].

These adhesive sites are distributed focally across the plasma membrane, spanning several square microns in area [11]. Cell signaling events at adhesive sites govern their formation and breakdown. This occurs through modulation of actin polymerization and filament contraction, which both contribute to cell motility [12-14]. Adhesive complexes assume the following distinct maturation forms based on location and morphology: nascent adhesion, focal contact, focal adhesion, and

fibrillar adhesion [15]. The adhesion lifecycle begins first with focal contacts forming at protrusions at the cell periphery during membrane ruffling. When the lamellipodium retracts, the focal contacts move towards the rear of the cell, growing in size to form large, plaque-like structures known as focal adhesions. Finally, focal adhesions can mature into fibrillar adhesions, which are characterized by a thin, thread-like morphology and increased amounts of the protein, tensin. Fibrillar adhesions are sites of extracellular matrix remodeling and form when cells have remained immobile for an extended period of time [14].

Throughout the adhesion lifecycle, these sites serve as signaling platforms, taking in environmental cues (both biochemical and mechanical) and relaying the information back to the cell through numerous enzymatic and adaptor proteins associated with the integrins. Integrins govern a complex signaling cascade with broad biological implications for cell homeostasis [16], embryonic development [17], tissue maintenance and repair, wound healing [18], and cell to cell contacts (e.g., immune synapse) [19]. Pathological effects are linked to the alteration or disruption of adhesion dynamics; for example, overexpression of integrins correlates to the metastatic potential of some human cancers [13-15].

1.1.2 Integrin structure and activation

Integrins are heterodimeric protein complexes composed of an alpha (α) and a beta (β) subunit. In humans, there are 18 α- and eight β- subunits which form 24 distinct integrin pairs with different binding properties and affinities for different ECM ligands such as fibronectin, collagen, or laminin [3, 19, 20]. Out of the 24 possible integrin heterodimers, β1 integrin subunits are the most widely expressed integrin subunit across cell types, partnering with various α-subunits to

form 12 unique heterodimers. The abundance and promiscuity of β1 integrins have overarching impacts on many cellular processes and physiology.

Integrins have large ectodomains, a single transmembrane helix in each subunit, and a short unstructured cytoplasmic tail. The α-subunit ectodomains consist of four or five subunits. The β-subunit has seven domains including the β-I domain, four epidermal growth factor (EGF) modules, and a tail domain. The α- and β-subunits meet at the interface between the α- subunit's β-propeller and β- subunit's β-I domain creating a binding site or cleft for ECM ligands.

The integrin ectodomains have been shown to exist in at least three different conformational states that determine their activation state as shown in Figure 1-2. [1, 19, 21-23]. In the inactive state, the large ectodomains bend in half towards the plasma membrane, with the binding cleft between the α- and β subunit closed off from the external ligand. In the active conformational state, the extracellular ectodomains are upright and extended and also characterized by physical separation between the α- and β- transmembrane subunits. The separation between their cytoplasmic tails leaves the tails exposed and provides docking sites for various cytoplasmic proteins involved in the integrin-signaling cascade. The third conformational state is an intermediate state between bent, inactive and fully extended, active. An upright ectodomain characterizes this state, but no physical separation between the α- and β- transmembrane subunits. Evidence also suggests that this extended, intermediate state does not bind external ligand [21]. The study of these conformational states as it relates to integrin signaling relies heavily on the development of monoclonal antibodies that detect conformational-dependent epitopes which have been instrumental in determining how the conformational state of the integrin impacts cytoplasmic binding partners and the downstream signaling cascade [24].

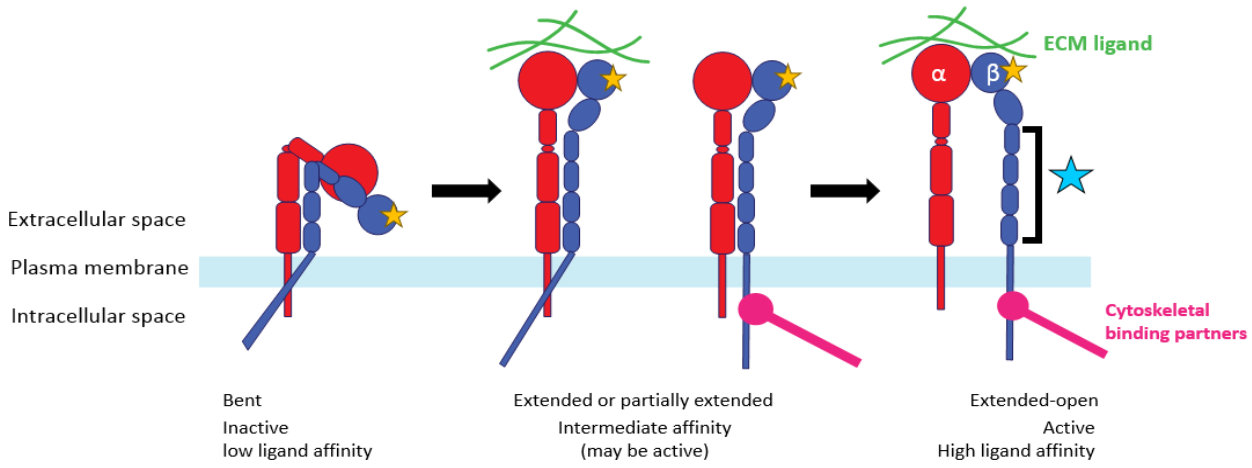

Figure 1-2 Integrin activation states

Representative schematic of integrin activation. Inactive integrins are characterized by a bent ectodomain that bends toward the plasma membrane (left). Conformationally active integrins have extended, upright ectodomains and physical separation between the transmembrane segments of the alpha and beta subunit. Intermediate states have characteristics of both inactive and active conformations, sometimes with a single binding partner (middle). Conformation specific antibodies can detect different activation states. Yellow star indicates an antibody that detects total integrin population, blue star indicates an antibody that recognizes active conformers. Figure adapted from [1-4].

Apart from the presence or absence of ligand which can control integrin activation, integrins can be further regulated by the presence of divalent cations at the β-I domain [1, 25, 26]. There are three cation binding sites present in the β-I domain, the first, the "metal-ion-dependent adhesion site" or MIDAS, is where Mg^{2+} binds promoting ECM ligand binding. MIDAS is flanked by two inhibitory Ca^{2+} binding sites, the "synergistic metal ion binding site" or SyMBS and the "adjacent to MIDAS" or "ADMIDAS." There are approximately 1mM Ca^{2+} and 1mM Mg^{2+} circulating the blood, which partner together to keep integrins in a basal level of activation or resting state. However, upon removal of Ca^{2+} or addition of the non-physiological stimulus, Mn^{2+}, integrins will rapidly activate, and form adhesion sites [27]. The interplay of ligand and cation

binding and detection through conformational specific antibodies has been used extensively to probe the structure-function relationship of integrins, including therapeutic drug and antibody design and deciphering the downstream signaling cascade through this "outside-in" activation of integrins.

Integrin activation can also be accomplished through the "inside-out" regulatory network of proteins and biomolecules in the "Integrin Adhesome" [9, 10]. This type of activation is of particular importance to leukocytes or hematocytes which circulate the blood in a low adhesive state before becoming fixed extracellular components to participate in immune function or wound repair. In this case, intracellular binding proteins, such as talins or kindlins, interact with the tails of the integrin β subunit disrupting the salt bridge connecting the α- and β- subunit's tails [28]. As mentioned previously, the separation of these tails increases affinity for ECM ligands, leading to sites of integrin extension, and the large-scale conformational changes in the integrin's ectodomains. Talins accomplish the salt-bridge disruption through a specific phosphotyrosine-binding (PTB) subunit on their FERM (Four-point-one-protein, Ezrin, Radixin, Moesin) domain. The PTB domain binds specifically to the membrane-proximal (MP) region of the β-tail, increasing the likelihood of tail separation. The FERM domain has several residues that interact with charged lipid species in the membrane. Similarly, kindlins also possess a membrane directing FERM domain with a unique pleckstrin homology domain that directs them to the membrane while also facilitating a binding interaction with the β-tail. Cell knockout studies have shown that talin is required for integrin activation and kindlin crosstalk mediates its function.

1.1.3 Talin and kindlin recruitment is influenced by plasma membrane levels of the lipid, Phosphatidylinositol 4,5-bisphosphate (PIP2)

Talins and kindlins have shown to contribute to integrin activation by binding directly with the cytoplasmic domain the β1 integrin tails by disrupting a salt bridge that locks the legs of the α and β integrin subunits together. To complete this action, the FERM domain of Talin must be unmasked or exposed, which can be accomplished through interactions with the lipid Phosphatidylinositol 4,5-bisphosphate (PIP2) in the plasma membrane [28-30]. PIP2 is an acidic, charged lipid that resides in the cytoplasmic leaflet of the plasma membrane. Regions of PIP2 have shown to anchor both talin and kindlin through interactions with their structurally similar FERM domains to the cytoplasmic leaflet of the plasma membrane [28, 31-33]. Additionally, PIP2 has shown to have more of a robust effect on talin by relieving its autoinhibited conformational state. Talin and kindlins co-activate integrins together by binding to the cytoplasmic tails [28, 29, 34, 35]. Evidence also suggests talin regulates PIP2 production levels through its interaction with phosphatidylinositol phosphate kinase type Iγ (PIPKIγ) [36, 37]. Finally, PIP2s have been proposed to sequester into lipid rafts or liquid-order domains, as evidenced through their sensitivity to cholesterol depletion or perturbations to membrane composition. [33, 38, 39].

Through either "outside-in" "inside-out" activation, integrin rapidly clusters moving laterally in the membrane to form adhesion complexes or sites. These sites then serve as hubs for cell signaling molecules that are associated with adhesion sites. The FAK-Src complex, a main mediator of cell signaling activity at adhesions, is discussed in the following section.

1.1.4 The FAK/Src signaling complex is hypothesized to be sensitive to membrane composition

Focal adhesion kinase (FAK) is a non-receptor tyrosine kinase that is recruited to clustered integrins in adhesive sites. It is one of the main mediators of the downstream signaling cascade,

particularly in the formation and breakdown of adhesive sites, and cell migration across many cell types [40-44]. FAK knockout studies resulted in a lethal phenotype in embryonic fibroblasts, demonstrating that FAK is required for early development and migration [45]. On the other extreme, overexpression of FAK is a characteristic of many tumors and is correlated to metastatic potential [46-48]. FAK's structure consists of an N-terminal FERM domain, kinase domain, two proline-rich stretches, and a focal adhesion targeting (FAT) domain. The FERM domain is similar to the one present in talin and kindlin and can interact with the β1 integrin tails or growth factors associated with adhesions. The C-terminal FAT domain has been proposed to help orient FAK to integrins and adhesions through interactions with focal adhesion components talin, paxillin, and vascular endothelial growth factor receptor (VEGFR) [49].

A closed conformation characterizes FAK's inactive state, wherein the FERM domain binds to the kinase domain closing off the tyrosine residue at position 397 (Y397) from autophosphorylation [41, 44, 50, 51]. When FAK's FERM domain interacts with β1 integrin cytoplasmic tails or other activators, the conformational change unmasks the Y397 site for autophosphorylation. This results in the exposure of a nearby "PxxP'' motif binding site for Proto-oncogene tyrosine-protein Src, abbreviated Src, to phosphorylate tyrosine residues 576 and 577 to fully activate FAK and transition into the FAK/Src signaling complex [51-54]. The activated FAK/Src complex initiates many downstream signaling pathways. This includes the phosphorylation CAS/Crk complex which helps regulate membrane ruffling and cell migration, activation of protease calpain which helps adhesion site turnover, the regulation of Rac-RhoA levels for cell spreading, the recruitment of the lipid kinase, Phosphatidylinositol-4,5-bisphosphate 3-kinase (PI-3K) to the membrane integrating PI-3k/Akt and MAPK/ERK pathways, and more [55, 56].

The downstream signaling cascade of a functional FAK/Src complex depends on their subcellular location and how they are recruited to the membrane [56-58]. As mentioned previously, FAK's subdomains associate with β integrin tails or focal adhesions complex proteins. Src's association with the membrane comes from the N-terminal myristoylation and polybasic amino acid site in its structure [44, 58]. Research indicates that these membrane-orienting characteristics of Src or other SFKs localize these kinases to lipid rafts or liquid-ordered domains [59, 60].

Adhesion site formation and the subsequent signaling cascade is tightly spatiotemporally controlled, and it is essential to have an understanding how the plasma membrane can help or hinder this process. In the next section, I review the plasma membrane environment and how the chemical structure and physical properties of lipids influence this organization.

1.2 Plasma membrane heterogeneity impacts cell organization and function

1.2.1 Cell membrane heterogeneity

The cell membrane is two-dimensional fluid composed of lipids and proteins. The first model describing this landscape with proteins incorporated into the bilayer was in 1972 by Singer and Nicholson [61]. The so-called fluid-mosaic model represented a surface of lipids, dotted with proteins across a homogenous lipid landscape. The movement of the membrane-associated proteins was governed by Brownian motion and mostly unrestricted. The surrounding lipids diffused similarly and were represented by a uniform distribution across the surface acting as a solvent [61]. In the following years, more evidence contradicting the simplicity of this model began to emerge. For instance, the diversity of membrane lipid species indicated the surface was not uniform [62, 63]. Studies on epithelial cells showed distinct differences in the lipid composition of the apical and basolateral membrane of these cells indicating both the diversity in

membrane architecture as well as linked lipid-protein directed movement [64, 65]. Moreover, the membrane environment has been shown to be incredibly dynamic and functionally diverse, contributing to maintaining cell integrity [66, 67], lipid signaling [68, 69], and regulation of membrane-bound proteins and traffic.

In 1997, Simons and Ikonen refined this model by proposing lipids be arranged into domains or "rafts" based on their chemical properties - including or excluding proteins – creating lateral heterogeneity across the membrane [65]. In this model two co-existing domains are represented, one with one domain dominated by saturated phospholipids, sphingolipids, and cholesterol, and the latter formed with unsaturated lipids. This lateral heterogeneity creates a diverse and dynamic plasma membrane landscape. The model further hypothesizes that associated membrane proteins can partition into specific domains, creating centers or platforms for cell signaling. The domains proposed by Simons and Ikonen to form on cell membranes are akin to the phase separation behavior observed in simple lipid mixtures and giant plasma membrane vesicles (GPMVs).

1.2.2 Phase separation and behavior in membranes

Lipids are seemingly simple structures - a hydrophilic, polar head group accompanied with hydrophobic, hydrocarbon tails. Their diversity emerges from varying head groups, charge, length of hydrocarbon tails, and number of double bonds [70]. In solution, lipids assemble to form bilayers which have different phase properties, dictated by the length and saturation of their hydrocarbon tails. Bilayers consisting of lipids with long, saturated hydrocarbon tails form solid or gel phases at room temperature [71-77]. In contrast, lipids whose hydrocarbon tails have some degree of unsaturation interfere with the hydrocarbon chain packing. As a result, the unsaturated lipids are unable to form a gel phase and form a more fluid, liquid-phase. The temperature at which

gel-phase lipids "melt" and form a two-dimensional fluid is defined as the phase transition or chain melting temperature. Phase transition also involves a significant change in both positional order and conformational order of the lipids in the membrane. The positional or translational order is a measure of lipid fluidity and related to the lateral diffusion coefficient. Conformational order refers to the fluidity of the tails themselves, specifically the *trans-gauche* isomerization of the chains [78].

In general, as the length of saturated hydrocarbon tails increases, the van der Waals interactions require more energy (or higher temperature) to break up the ordered packing of the gel phase. Similarly, the unsaturated chains of the liquid phase need a much lower temperature to restrict the movement of the tails enough to create the ordered packing of the gel phase. In bilayer binary mixtures, two phases can coexist in spatially separate populations when the components have different chain melting temperatures. Immiscibility is not limited to systems with lipids in the extreme lipids phases (gel or liquid), phase separation can also occur in two liquid phases. The intersection of two liquid-liquid phases is of particular importance for understanding the cell membrane, a two-dimensional fluid [79].

The fluid phase described previously is also known as the liquid-disordered (L_d) phase characterized by the loss of extended lipid chains and order of the gel-phase. The liquid-disordered phase has been shown to regain some order, while maintaining its fluidity, in the presence of sterols which impacts the packing of the acyl chains. This liquid-ordered phase (L_o) shares both gel-like and fluid-like characteristics. Stiff planar sterols, like cholesterol, intercalate the lipid bilayer, influencing the lipid chains to favor a *trans*- conformation. As a result, the liquid-ordered phase exhibits positional order and lateral diffusion like the fluid phase [80, 81], but conformational order like the gel phase [72, 82, 83]. Coexistence of these two particular phases is defined by the

separation of saturated (liquid-order favoring) and unsaturated (liquid-disorder favoring). Sorting of membrane lipids into the liquid-ordered and disordered phase is dependent on the chemical structure of the lipids. Saturated phospholipids, sphingolipids, and glycolipids sort into the liquid order phase, while unsaturated lipids align with the disordered phase.

Lipid phase behavior has been proposed to be a core physical contributor to the organization of the plasma membrane. The aforementioned "raft hypothesis" proposes that physical properties and interactions of lipids that generate phase separation in simple lipid mixtures also form similar nano-domains in the cell. In these nano-domains, order-preferring or disorder preferring lipid associated with each other, and can be stabilized by protein-protein and protein-lipid interactions, like those hypothesized to form through integrin-mediated adhesion. The link between integrin-mediated adhesion and membrane order is discussed in the following section.

1.2.3 Integrins and adhesive complexes are sensitive to membrane composition

At least two major lipid components of biological membranes associated with membrane order have shown to interact with integrins directly: cholesterol and sphingolipids. Cholesterol has been shown to affect both adhesion complex formation and the downstream signaling cascade. Increasing cholesterol was reported to cause the fibronectin receptor integrin, α5β1, to cluster and form adhesive complexes more rapidly and a stronger binding interaction with fibronectin [84]. Another study by Ramprasad and colleagues noted that depletion of cholesterol from the plasma membrane in cells caused rapid disassembly of adhesive complexes and reduced focal adhesion kinase activity when cells were plated on fibronectin, and not laminin, vitronectin, or plastic [85, 86]. These data demonstrate cholesterol effects fibronectin-binding integrins including α5β1, as well as other β1, β3, and β5 subunit containing heterodimers. Cholesterol has also been shown to

be essential for the function of the αvβ3, CD47, and G- protein signaling complex, and upon depletion of cholesterol it fails to form entirely [87]. Introduction or depletion of sphingolipids has also reported having a similar effect on integrin-mediated adhesion. Sphingomyelinase (SMase) activity which reduces sphingomyelin (SM) levels in cells was shown decrease integrin-mediated adhesion and hinder integrin mobility [88]. The addition of C8-lactosylceramide (C8-LacCer) to the plasma membrane, initiated clustering in active β1 integrins and formation of adhesive complexes, coupled with increased integrin signaling and reorganization of actin [89]. These studies emphasize how membrane composition and environment have a profound effect on the functionality of integrins or adhesion complexes. The underlying mechanism for how integrins sequester into membrane domains remains unclear, but it assumes balance exists between membrane phase behavior and functionality of integrin-mediated adhesion.

Several microscopy studies link active integrins or clustered integrins in adhesions to regions of membrane order or "lipid rafts" [60, 90-98]. Single molecule studies utilizing near-field scanning optical microscopy (NSOM) by van Zanten and colleagues demonstrated that leukocyte integrins co-localize or are proximal to domains of membrane order marked by glycosylphosphatidylinositol-anchored proteins (GPI-AP) [95]. Confocal spectroscopy XY scanning by Siegel and colleagues on model membrane bilayers demonstrated the integrins, $\alpha_v\beta_3$ $\alpha_5\beta_1$, partition to liquid-disorder domains in the absence of ligand (fibronectin or vitronectin)[99]. Upon ligand binding, results indicated a substantial shift of integrin partitioning to liquid-order domains without oligomerization or clustering of the receptors, in the absence of cytosolic proteins. A study by Gaus and colleagues found that integrin-mediated adhesion sites were ordered environments through the use of the fluorescent membrane probe, Laurdan [100]. Laurdan measures membrane packing or order by measuring the extent of water penetration or permeability

across the membrane. It does not preferentially partition into any membrane environment, but it does undergo a different spectral shift in regions of membrane order. Finally, a study by Seong and colleagues demonstrated using a fluorescent biosensor that the adhesion associated kinase, Focal Adhesion Kinase (FAK), was more active in liquid-ordered or "lipid raft" domains than in non-raft regions across the plasma membrane. They concluded that FAK is activated in the liquid-ordered regions, and provide evidence that adhesions are rich with liquid-ordered membrane domains [101, 102].

Although significant headway has been made to answer the question of how integrins interact with lipid phase heterogeneity as part of their signaling response, the impact of lipid phase behavior on signaling is intrinsically difficult to study in cells because the phase heterogeneity is proposed to exist as short-lived nanodomains. The development of higher resolution imaging techniques, like super-resolution microscopy, have given a new promise to directly visualizing the impact of lipid heterogeneity in the plasma membrane.

1.3 Super-resolution microscopy maps spatial distribution of lipids within integrin-mediated adhesion

1.3.1 Principles of super-resolution microscopy

Classical optical microscopy provides numerous methods to visualize protein-lipid interactions, but the spatial resolution of these microscopes is limited to half the wavelength of light (approximately 250nm). This spatial resolution restriction has hindered visualization of biological interactions at the sub-diffraction scale. Two recent advancements in fluorescent localization microscopy: (direct) stochastic optical reconstruction microscopy (STORM/dSTORM) [103, 104] and photo-activation localization microscopy (PALM) [105, 106] have improved resolution by an order of magnitude. In general, these techniques overcome

the diffraction limit barrier by exploiting the photo-conversion behavior of fluorescent dyes or small proteins.

Conventional fluorescent microscopy collects data from all the emitting fluorophores at once, blurring the fine detail of the underlying structure. In STORM and PALM approaches, biological samples are densely labeled with fluorescent molecules that stochastically blink between fluorescent and dark states continuously under the right buffer conditions. Images are collected continuously over time, collecting images of only a subset of the probes at each snapshot instance. Once enough images are collected so that the entire set of fluorophores have been well sampled, each localization is precisely fit with a 2D Gaussian. A reconstruction image from this information sums all the localizations together, giving a spatial map of all the fluorophores across the sample. By fitting each diffraction-limited spot individually, the fine structure of the underlying sample is revealed with resolution at 10 - 20nm. Localizations from fluorophores targeting proteins and lipids simultaneously the can be analyzed to determine their relationship and length scale of their correlation, providing a map of the protein-lipid interactions across the cell.

1.3.2 Super-resolution studies reveal new functional roles of adhesion-associated proteins

Super-resolution microscopy approaches have already proven to be instrumental in uncovering the intricacies of integrin-mediated adhesion. Recently, the nanoscale 3-D organization of integrin-based adhesions was determined through super-resolution microscopy. Results from these experiments were able to determine the precise location of adhesion-related proteins in 10-15nm resolution. These images characterize that focal adhesion kinase, talin, and paxillin reside closest to the integrin tails while vinculin, zyxin, and vasodilator-stimulated phosphoprotein (VASP) reside closer to actin, revealing new potential protein-protein interactions based on their

proximity to each other [107]. Knowing their precise location also sheds more light on the roles they play in the adhesion, i.e., scaffolding or force transduction in cells. Results from Rossier and colleagues demonstrated that β1 and β3 integrins take on different roles in adhesions and that the life cycle of adhesion sites is remodeled in less than 100 seconds [108]. Another study used a FRET-based sensor and super-resolution microscopy to determine that αvβ3 integrins localized to regions of high force and revealed a new role for paxillin in force transmission at adhesions [109]. In sum, the application of super-resolution imaging techniques reveals features of integrin-mediated adhesions that remained elusive in diffraction-limited microscopy. Most importantly, super-resolution microscopy gives researchers a platform to study integrins, adhesions, or associated signaling components in their native membrane environment in living or fixed intact cells.

1.4 Current studies and dissertation outline

The past forty years studying integrin-based adhesions has laid out an extensive foundation of knowledge for understanding the composition, morphology, and downstream signaling cascade emitted from these structures. It is evident that their microenvironment spatiotemporally controls their life cycle and they are sensitive to chemical and mechanical perturbations. However, there is a lack of understanding how the cell membrane, specifically lipid composition, heterogeneity, and lipid physical properties can impact integrin biology. The work presented in this thesis uses super-resolution microscopy to measure the interactions between integrins and peptides with membrane phase preference in intact cell membranes. This is motivated by the increasing evidence of the effect cell membrane heterogeneity has on membrane-associated proteins and their downstream signaling cascade.

In Chapter two, two-color super-resolution localization microscopy is employed to create high spatial resolution maps of β1 integrin-mediated adhesion and protein markers of membrane phases in mouse fibroblasts. Cross-correlation analysis is used to quantify the relationship between β1 integrins and membrane markers after adhering to fibronectin for one or 24 hours. A density-based algorithm is applied to reconstructed images to determine membrane order preference of integrins found inside and outside adhesive sites. Results from this study show that integrins found in mature fibrillar adhesions have the strongest association with membrane order.

In Chapter three, conformation-specific antibodies are used to determine how active β1 integrins are distributed across adhesive complexes. Adhesions are found in mosaics, composed of integrins in at least two conformational states. Methods and analysis from Chapter two are employed to determine that active-conformation integrins do not exhibit a stronger preference for membrane order versus the total β1 integrin population. Finally, I show that biochemical membrane perturbations, long chain *n*-alcohols, can bias integrin activation state and adhesion complex.

In Chapter four, I provide a summary of all my results and conclude that β1 integrin-mediated adhesion is sensitive to membrane composition, but not a result of conformationally active β1 integrin's association with membrane order. My results support a model that β1 integrins are indirectly impacted by membrane order, likely through the regulatory networks responsible for "inside-out" signaling.

Chapter 2: The Spatial Distribution of Lipids in β1 –Integrin-Mediated Adhesion

2.1 Chapter Overview

Integrins are transmembrane adhesion receptors that partner with ligands in the extracellular matrix and cytoskeletal proteins to oligomerize, resulting in multi-protein adhesive complexes. Integrin functionality is hypothesized to be sensitive to cell membrane composition, driven at least in part by the tendency for the plasma membrane to separate into ordered and disordered domains resembling the coexisting liquid phases observed in model membranes. In this chapter, two-color super-resolution microscopy is used to quantify the local membrane environment surrounding β1 integrins by tabulating cross-correlations between antibody labeled β1 integrins and expressed peptide markers of ordered and disordered phase-like domains expressed in intact cells. Current views on integrin clustering hypothesize membrane composition helps the formation of adhesive complexes during cell attachment or cell spreading. However, from my results, I conclude that clustered β1 integrins from mature, fibrillar adhesive complexes have a stronger preference for membrane order than their earlier maturation adhesion complex counterparts.

2.2 Introduction

Integrins are transmembrane adhesion receptors that connect the extracellular matrix (ECM) to the actin cytoskeleton. Integrins are heterodimeric protein complexes composed of an alpha (α) and beta (β) subunit. There are 18 α- and eight β- mammalian subunits which form 24 distinct integrin pairs with different binding properties and affinities for different ECM ligands [1, 7, 19]. In particular, the β1 subunit is the most widely expressed in cell types, partnering with various α-

subunits forming 12 of the 24 distinct pairs. The β1 integrin subunits are abundant and promiscuous, and their activity mediates biological events across many signaling pathways [110].

Integrins are mobile and diffusely distributed across the membrane before activation. In general, integrin activation occurs when integrins undergo a conformational change from a low affinity (bent) state to a high affinity (upright or extended) state. Evidence also supports the existence of intermediate states, with different conformations and affinity for a ligand or intracellular binding partners [19, 21]. Integrins are capable of signaling bidirectionally across the membrane, which is dependent on this conformational change [1, 19, 21, 23].

Adhesive complexes or contacts form when integrins activate, cluster and bind with extracellular ligands and cytoskeletal proteins to form dense, micron-sized multi-protein complexes. The complexes are distributed focally across the membrane, serving as both mechanical anchors for the cell and signaling hubs. Integrin signaling governs events that are critical for maintaining proper cell growth, morphology, and viability [1, 6, 7]. The formation of adhesive complexes, changes in integrin conformation, and recruitment of associated adhesion signaling proteins have been proposed to be sensitive to the lipid composition of the plasma membrane [60, 84-98]. This is hypothesized to be influenced by the ability of the plasma membrane to segregate its components laterally into nanodomains of uniform composition, commonly referred to as the "lipid raft" hypothesis. The "raft" is a membrane domain, rich in saturated acyl chain lipids, and cholesterol that resembles the liquid-ordered (L_o) membrane phase. This liquid-ordered region is surrounded by more fluid unsaturated lipids that resemble the (L_d) phase.

Evidence supporting “lipid raft” hypothesis stems from our current knowledge of the plasma membrane landscape and the ability for lipids to self-assemble. The membrane environment is diverse, not only in the proteins embedded or associated with it, but with the molecular diversity of the lipids themselves - from varying head groups, charge, length of hydrocarbon tails, and number of double bonds[65, 74, 79, 111]. Lipids are capable of self-assembly based on their composition in the presence of cholesterol, which is thought to compartmentalize proteins to help or hinder their ability to function. This is of particular importance for receptors that cluster to elicit a cellular response, like integrin-mediated adhesion, B Cell receptor [112-117] or T Cell receptor signaling [118-120].

One of the main barriers to directly visualizing membrane-mediated activity in intact cells is that these interactions are hypothesized to take place at length scales out of reach from conventional optical microscopy. However, sub-diffraction super-resolution imaging techniques can be adapted to provide high spatial resolution maps of the plasma membrane and provide evidence for the existence of phase-like domains in intact cells [112, 113].

This study presented in this work uses dual color super-resolution fluorescence localization microscopy to determine the nanoscale organization of β1 integrins and peptide markers of membrane phases within the plasma membrane of primary mouse embryonic fibroblasts and human metastatic breast cancer cells. I report the total population of β1 integrins, independent of conformational state or adhesion association, co-localizes with peptides that mark both liquid-order and disorder phases. I identify that integrins that have clustered to form mature adhesive complexes co-localize with markers of membrane order through the application of a density-based cluster algorithm. I conclude from these data that β1 integrin’s preference for membrane order depends on its conformational state and may be required for integrin-mediated cell signaling.

2.3 Results

2.3.1 Integrins co-localize with both liquid-order and liquid-disorder membrane probes

Membrane heterogeneity was monitored through imaging the spatial distribution of membrane-anchored peptides around β1 integrins in primary mouse emybronic fibroblasts (MEFS). The peptides used in these study have previously been shown to mark liquid-ordered or liquid-disordered phases in isolated plasma membrane vesicles and ordered and disordered phase-like domains in intact cells.[112, 121, 122]. Liquid-ordered domains were marked with PM, a mEos3.2 photoactivatable fluorescent protein lipidated through saturated palmitoyl and myristoyl modifications from the 11 N-terminal residues of the Tyrosine-protein kinase, Lyn. Liquid-disordered domains were marked with TM; a mEos3.2 photoactivatable fluorescent protein-tagged attached to a short transmembrane peptide. The transmembrane sequence is derived from a 36-residue helix from the Linker -for-Activation-of-T-Cells (LAT) protein, with the palmitoyl sites, removed. PM and TM do not contain known motifs for protein-protein interactions, so their distribution is dependent on their interactions with their surrounding membrane environment. Cells are transiently expressing either PM or TM peptides adhered to fibronectin for one or 24 hours before chemical fixation and antibody labeling of total β1 integrins as described in Materials and Methods. The lateral distribution of both probes was measured through simultaneous stochastic optical reconstruction microscopy (STORM) [103, 104] and photoactivation localization microscopy (PALM) [105, 106], representative images are shown in Figures 2-1 and 2-2.

Reconstructed images are used to compute the cross-correlation of β1 integrin and PM or TM localizations across the whole cell area. The cross-correlation represents the average relative density between two probes as a function of the distance between them. On the cross-correlation

plot a value of 0 is normalized to represent the average density, this means for a value of 0.25 there is a 25% enrichment of that probe above the average at a specified distance.

Cell fixation and staining after one-hour captures integrin behavior during the rapid formation of adhesive complexes during cell spreading. Qualitatively, from the reconstructed images (Figure 2-1, panels A and B), the diversity of size, shape, and distribution of adhesions across the plasma membrane is evident. Cross-correlation analysis at this time point indicates total β1 integrin population, i.e., including all conformations present at the time of cell fixation, are similarly correlated with both liquid disordered and liquid ordered probes. This result indicates that β1 integrins – independent of activation conformational state or clustered adhesion site – recruit both markers of order and disordered domains. It also calls for further analysis to determine whether sub-populations of β1 integrins, specifically those found in adhesive complexes, have different affinity for order or disordered environments.

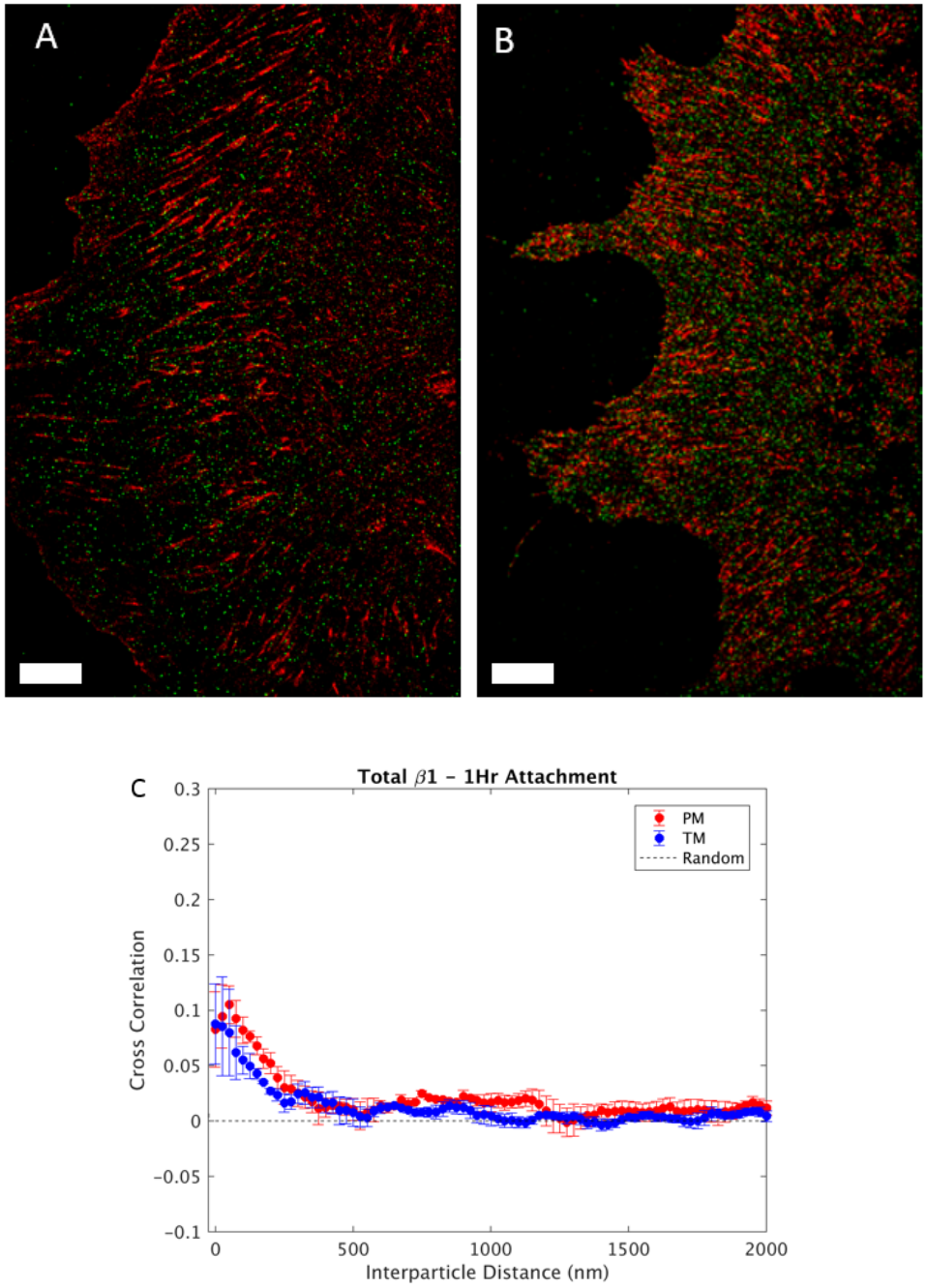

Figure 2-1: Cross-correlation between total β1 integrin population and membrane probes at 1-hour attachment.

A) Representative reconstructed image of total β1 integrin content (red) and PM (green) membrane probe localization in chemically fixed cells. Scale bar 5μm. B) Representative reconstructed image of total β1 integrin content (red) and TM (green) membrane probe. Scale bar 5μm C) The average cross-correlation between total β1 integrin and PM or TM after adhering to fibronectin for 1 hour. Errorbars reflect the standard error of the mean. Four cells were imaged and quantified.

Cell fixation at 24 hour attachment captures integrin behavior when the majority of the adhesion complexes present have matured into fibrillar adhesions [14]. Qualitatively, the images show the formation of large, more mature fibrillar threadlike adhesive complexes, some of which span over 10μm (Figure 2-2, panels A and B). This allows examination of the membrane environment with the presence of more structure, which might stabilize a heterogeneous membrane composition. Cross-correlation analysis of these cells reveals that at short length scales (less than 500nm) PM and TM are both correlated with β1 integrins, but PM with a slightly higher maximum correlation. Interestingly, PM continues to show correlation with β1 integrins out to 2μm, indicating there are long stretches, i.e., across the adhesive complex that correlate with the order-preferring membrane probe.

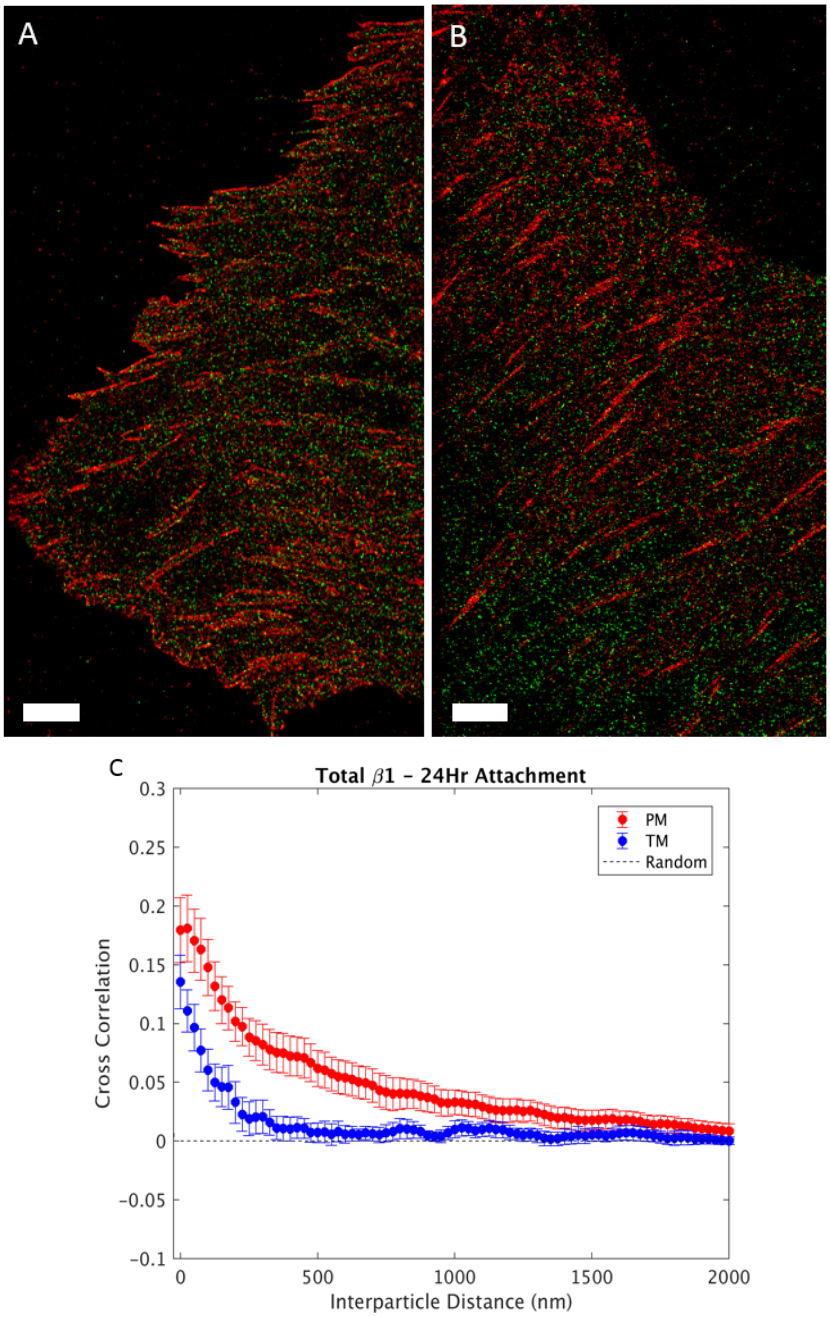

Figure 2-2: Cross-correlation between total β1 integrin population and membrane probes at 24-hour attachment.

A) Representative reconstructed image of total β1 integrin content (red) and PM (green) membrane probe localization in chemically fixed cells. Scale bar 5μm. B) Representative reconstructed image of total β1 integrin content (red) and TM (green) membrane probe. Scale bar 5μm C) The average cross-correlation between of total β1 integrin and PM or TM after adhering to fibronectin for 24 hours. Errorbars reflect the standard error of the mean.17 cells were imaged and quantified.

In summary, these data show a correlation between β1 integrins and membrane probes with conflicting membrane phase preference during cell spreading (Figure 2-1). At longer attachment times and as the adhesive complex matures, I see an emergence of a stronger correlation between β1 integrins and an ordered membrane environment. However, the marker of a disordered membrane composition is still present at short distances. I conclude from these data that β1 integrins do not preferentially sort into a domain of one distinct lipid composition, i.e., liquid-order or liquid-disorder. They seem to surround themselves with a mixture of different lipid compositions. I further conclude that additional analysis and experimentation is needed to determine if β1 integrins in different conformational, activation or adhesive complex maturation state might have different affinities liquid-ordered or liquid-disordered membrane domains.

2.3.2 Density-based clustering algorithm segments integrins to adhesion complexes

The antibody labeling scheme labels all β1 integrins including those not in clusters of adhesive complexes. To delineate between integrins in adhesive and non-adhesive complexes, the DBSCAN (Density-Based Spatial Clustering of Applications with Noise) algorithm is applied to the reconstructive images as described in Materials and Methods [123, 124]. DBSCAN operates by counting the number of localizations in a user-defined radius and applying a minimum localization or point threshold to determine a cluster. DBSCAN identifies localizations corresponding to integrins found inside and outside of adhesive complexes (Figure 2-3).

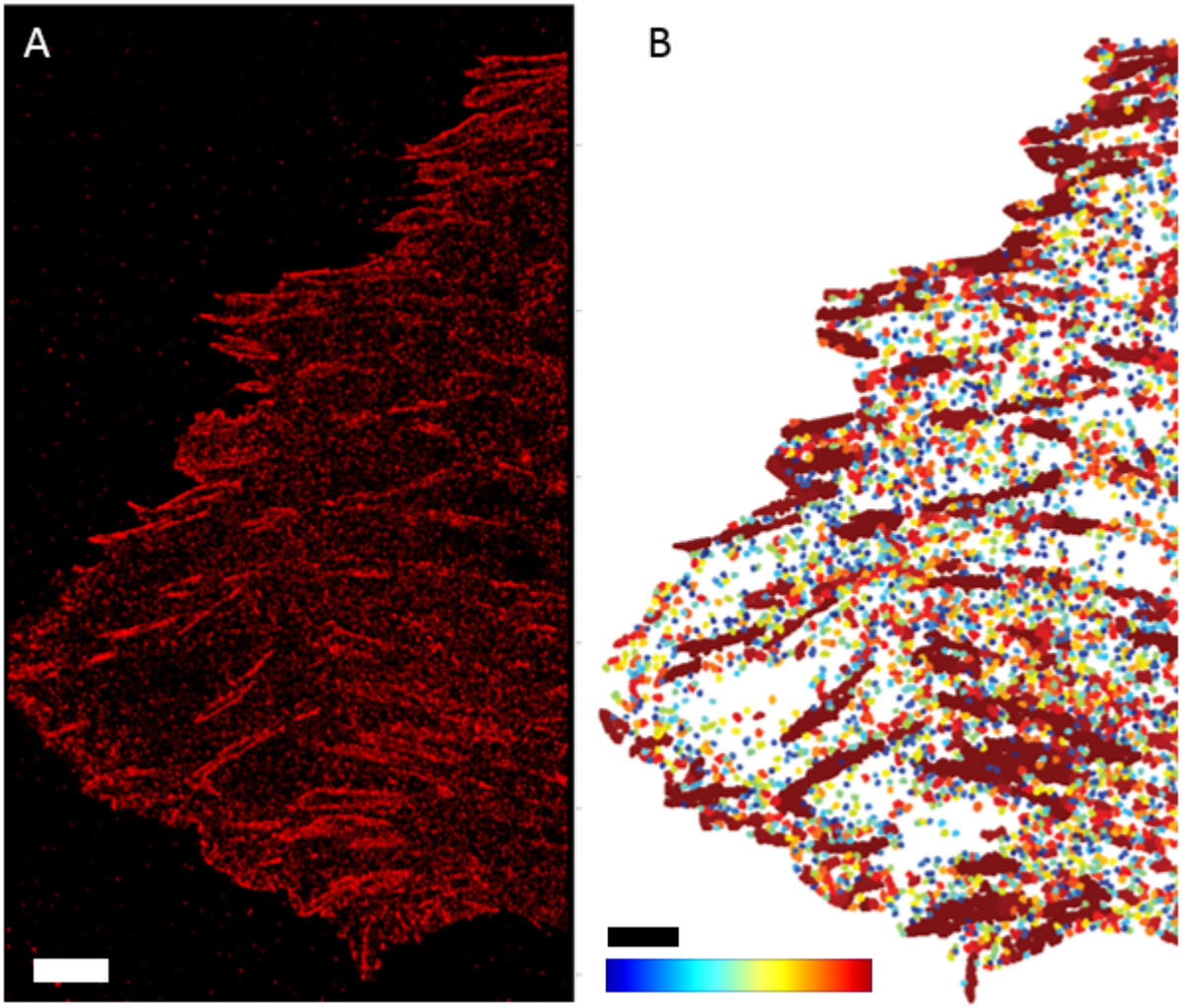

Figure 2-3: DBSCAN segmentation of β1 integrin localizations into clustered adhesions

A) Reconstructed image of the β1 integrin localizations after adhering to fibronectin for 24 hours. Scale bar is 5μm. B) Segmentation after passing the data through DBSCAN, cluster radius was set to 100nm, with a minimum point threshold set to ten. Black scale bar is 5μm. Color dictates the size of the cluster, where cooler colors represent the smallest clusters and warmer colors represent the larger clusters.

DBSCAN assigns each point localization to a cluster so that a reconstructed image can be dissected into different layers based on cluster size or a minimum number of points per cluster. In this particular case, the radius was set to 100nm and ten points minimum for each cluster. This allows a straightforward method to assign localizations inside or outside adhesive complexes (Figure 2-4). Any cluster larger than 1μm, on their long axis, is considered to be an adhesion.

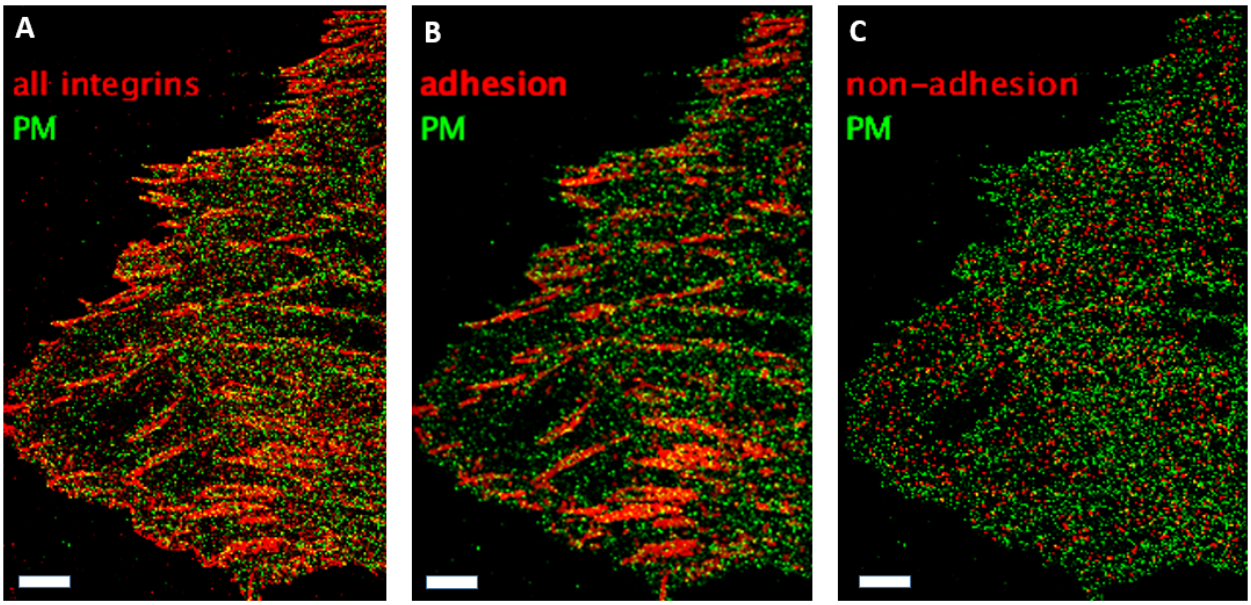

Figure 2-4: Segmentation of reconstructed images classifies localizations into adhesions

A) Reconstructed image of all β1 integrins B) Adhesion associated β1 integrins C) Non-adhesion associated β1 integrins. All scale bars are 5μm. Clusters larger than 1μm, on their long axis, are considered to be adhesions. Contrast across the panels is not consistent to highlight relevant features.

2.3.3 Mature adhesions are regions of membrane order

Cross-correlations between segmented β1 integrins and PM or TM were then computed at 1 hour and 24-hour attachment (Figure 2-5 and 2-6). Within error, I cannot conclude that adhesion-associated integrins have a stronger preference for liquid order over liquid disorder and vice versa. I conclude that β1 integrins during cell spreading and attachment associate with both markers of

membrane order and do not partition into a liquid-ordered membrane domain at this time point. However, at 24 hours, PM is more correlated with β1 integrins within segmented adhesive complexes than it is with integrins outside of the complexes. In contrast, TM exhibits the same magnitude and range of correlations with integrins independent of its adhesive complex association. This indicates that both membrane peptides associate with β1 integrins, but only the PM peptide is recruited to adhesions. Since PM is a marker of ordered lipid domains, this is consistent that the mature adhesive complexes are regions of membrane order. I conclude from Figures 2-5 and 2-6 that the fibrillar adhesions that emerge when cells have attached for long periods have the highest affinity for regions of membrane order in β1 integrin-mediated adhesion.

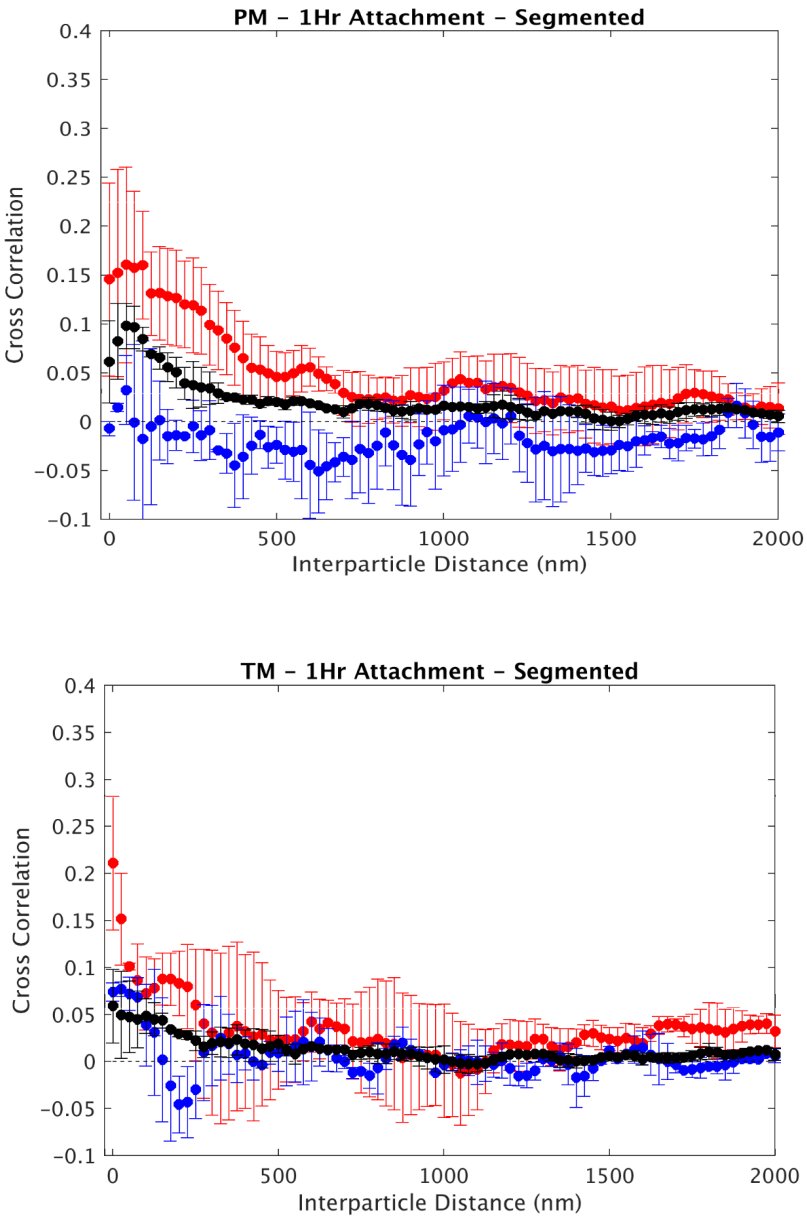

Figure 2-5: Cross-correlation plots at 1-hour attachment segmented for adhesions in MEFs

A) Cross-correlation between PM and adhesion-associated β1 integrins (red), non-adhesion associated β1 integrins (blue), and all β1 integrins (black). B) Cross-correlation between TM and adhesion-associated β1 integrins (red), non-adhesion associated β1 integrins (blue), and all β1 integrins (black). Error bars reflect the standard error of the mean. Four cells were imaged and quantified.

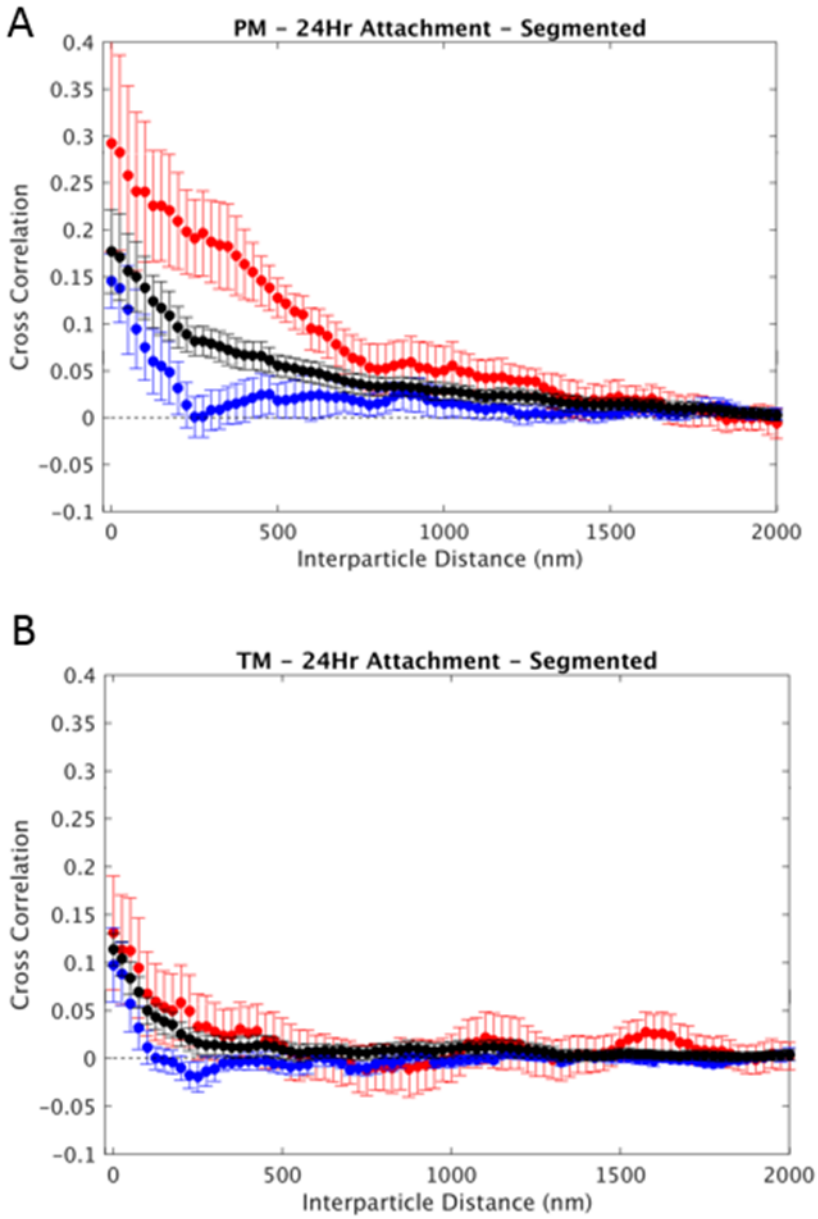

Figure 2-6: Cross-correlation plots at 24hour attachment segmented for adhesions in MEF cells

A) Cross-correlation between PM and adhesion-associated β1 integrins (red), non-adhesion associated β1 integrins (blue), and all β1 integrins (black). B) Cross-correlation between TM and adhesion-associated β1 integrins (red), non-adhesion associated β1 integrins (blue), and all β1 integrins (black). Errorbars reflect the standard error of the mean. 17 cells were imaged and quantified.

2.3.4 Local cross-correlation analysis confirms mature adhesions are ordered

During migration or cell attachment, adhesive complexes are continually forming and breaking down. This results in adhesions of different shapes, sizes, and orientations distributed focally across the membrane. One consequence of the cross-correlation analysis is averaging across the whole cell can wash out or de-emphasize some of these features of the adhesive complexes. Segmentation of the β1 integrin localization allows for a different approach to computing the cross-correlation between the integrins and membrane probes. In this approach, the local cross-correlation is computed by first identifying the adhesions through DBSCAN, confining it to a box of fixed size ($16\mu m^2$), computing the cross-correlation within in this area, and averaging the cross-correlation data amongst all the adhesions.

Figure 2-7 plots the 24-hour attachment result in both the cross-correlation across the whole area of the cell (panels A and B), and the computed local cross-correlation in the area of fixed size (panels C and D), not adjusting analysis for adhesion orientation. Here, areas of correlation or enrichment of a membrane probe are yellow, areas of anti-correlation or depletion of a membrane probe are blue, and teal represents a heterogeneous mixture. In comparison of the two-dimensional cross-correlations of PM result in panels A and C of Figure 2-7, it is evident that by averaging the cross-correlation across the whole area of the cell, some of the underlying structure is washed out as represented in the two-dimensional visualization. Regardless, the magnitudes of the computed cross-correlations (panels A and C, right) are in good agreement. For the TM result Figure 2-7 panels B and D, the center of the two-dimensional visualization shows hardly any correlation, and more like of random, mixed lipid mixture.

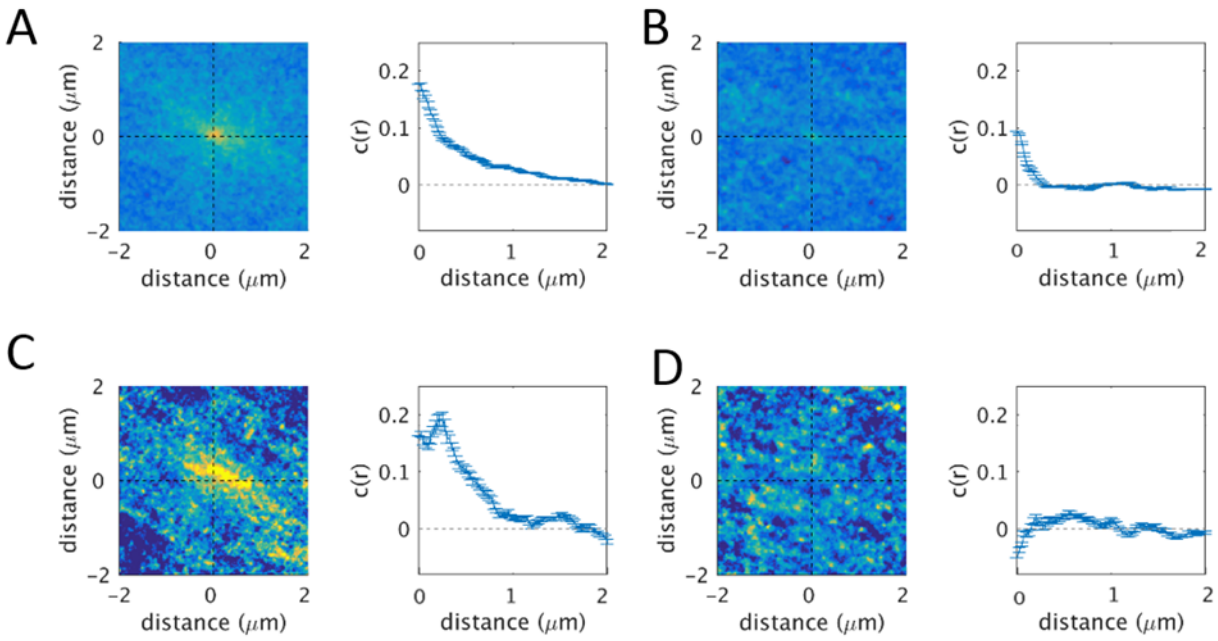

Figure 2-7: Local cross-correlation analysis results

Each panel displays a two-dimensional visualization of the cross-correlation and cross-correlation plot. A) Cross correlation of PM and total β1 integrin localizations B) Cross correlation between TM and total β1 integrin localizations C) local cross-correlation analysis of PM and total β1 integrin localizations D) local cross-correlation analysis of TM and total β1 integrin localizations.

In Figure 2-8, the local cross-correlation analysis is performed, but all the adhesions are centered and oriented in the same direction before averaging. Panels A and B are the two-dimensional visualizations of the cross-correlation, and panels C and D are their respective cross-correlation plots taken in the micron-sized area, confined by the horizontal white dotted lines. Here, the correlation between PM and β1 integrins is again evident, and the result between TM and β1 integrins is more like of random, heterogeneous lipid mixture. Each of these different approaches to computing the cross-correlation is in good agreement with each other and support my conclusion that mature, fibrillar adhesions are regions of membrane order.

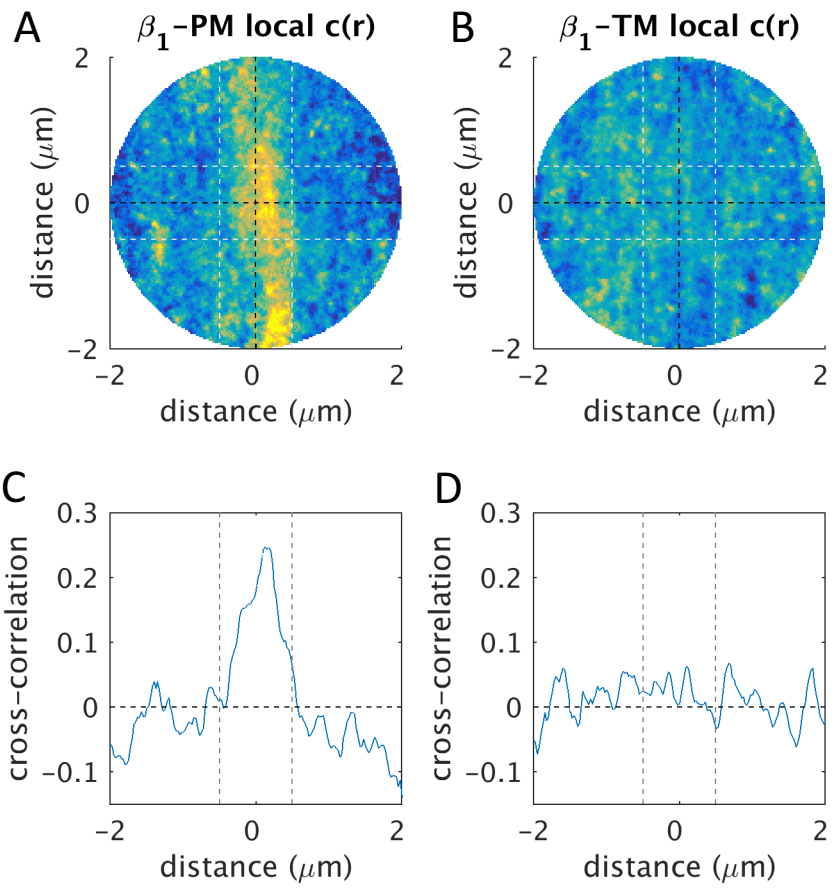

Figure 2-8: Local cross-correlation after the adhesion alignment at 24-hour attachment in MEF cells

Two-dimensional visualization (panels A and B) of the cross-correlation and corresponding cross-correlation plots (panels C and D) for the horizontal area bounded between the two white dashed lines. The order preferring probe, PM, is represented in panels A and C. The disorder-preferring probe, TM, is represented in panels B and D.

2.3.5 Adhesive complexes in metastatic breast cancer lines are regions of membrane order

Changes in lipid composition have been linked to cancer malignancy and metastatic potential in human cancers, such as lung, liver, and breast cancer [20, 110, 125, 126]. In breast tissue, it has been reported that healthy tissue has much higher levels of polyunsaturated fatty acids compared to cancerous tissue [127]. Additionally, others have reported that metastatic breast cancer cell lines have higher levels of saturated lipids and cholesterol, and are hypothesized to impact cell-adhesion machinery. In the next set of experiments, I sought to see if the membrane order trends observed in fibroblasts translated into an immortalized epithelial cell line. Here, the sorting of lipid-phase marker peptides is examined in highly metastatic breast cancer cell line, MDA-MB-231. The monoclonal mouse anti-human β1 integrin antibody, clone 12G10, was used to detect active conformation integrins and adhesive complexes in MDA-MB-231 cells, due to lack of a total β1 integrin population antibody suitable for immunofluorescence. Liquid-order domains were detected through PM-mEos3.2 and liquid-disorder domains through TM-mEos3.2. The lateral distribution of both probes was measured through simultaneous stochastic optical reconstruction microscopy (STORM) [103, 104] and photoactivation localization microscopy (PALM) [105, 106], representative images are shown in Figure 2-9.

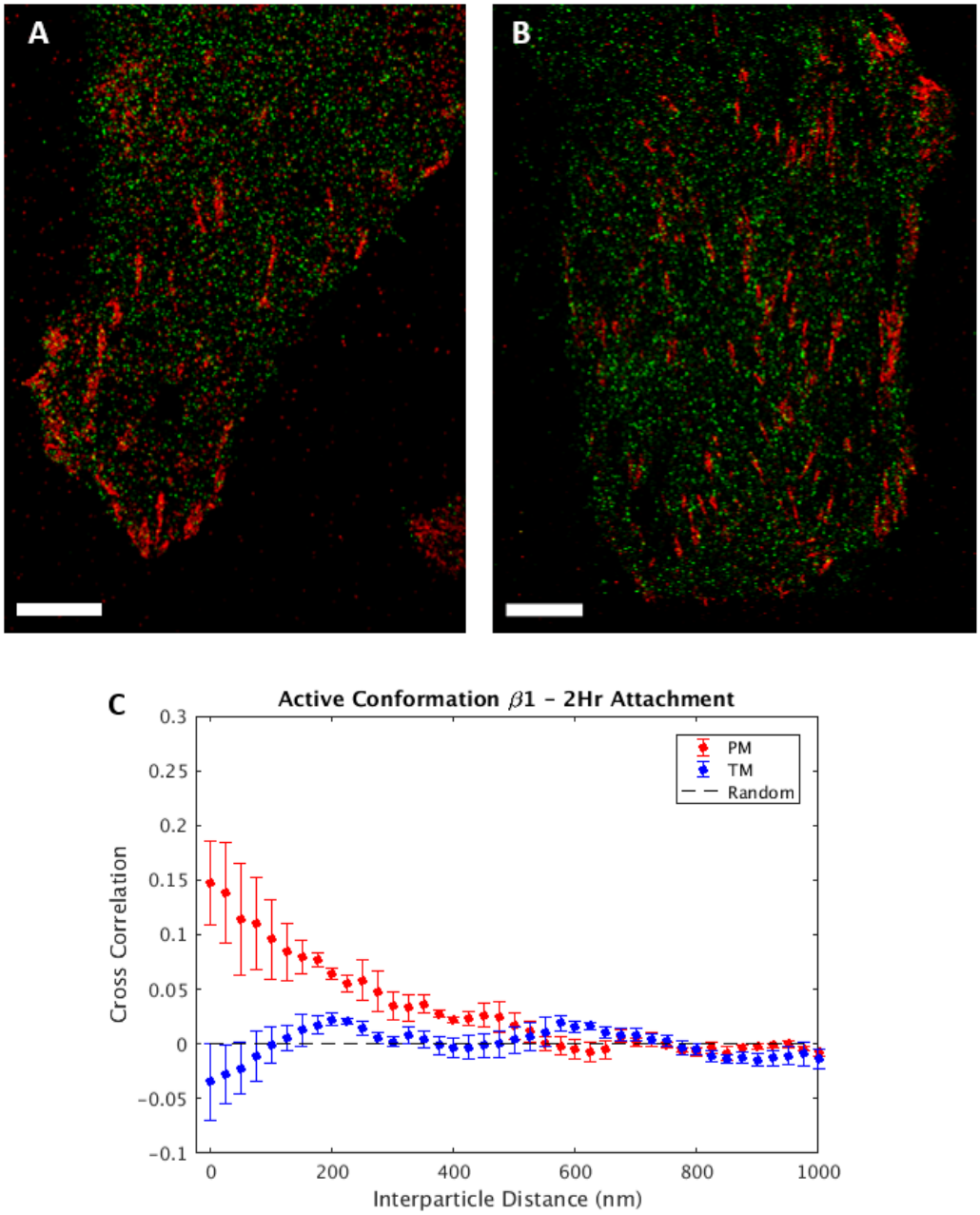

Figure 2-9: Cross-correlation between active β1 integrin population and membrane probes at two hr attachment in MDA-MB-231 cells

A) Representative reconstructed image of active β1 integrin content (red) and PM membrane probes (green) localization in chemically fixed cells. Scale bar 5μm. B) Representative reconstructed image of total β1 integrin content (red) and TM membrane probes (green) localization in chemically fixed cells Scale bar 5μm C) The average cross-correlation between of total β1 integrin and PM or TM after adhering to fibronectin for 2 hours. Errorbars reflect the standard error of the mean. Seven cells were imaged and quantified. Color balance adjusted to highlight adhesion features in reconstructed images.

MDA-MB-231 cells were plated on fibronectin and allowed to attach for two hours. Qualitatively from the reconstructed images (Figure 2-9, panels A and B), all the integrins are localized to adhesions which contrasts what I saw before. This is due to only targeting active-conformation integrins. The active β1 integrins co-localized the order-preferring probe, PM, at a maximum of 15%, and the disorder-preferring probe, TM, exhibits slight depletion on average at short distances, but predominately doesn't deviate from the average probe density across the cell. These results indicate that adhesions in two different cell types exhibit characteristics of membrane order. From these data, I conclude that active β1 integrins demonstrate a preference for membrane order and that further experiments in mouse fibroblasts are needed to determine how conformational state impacts integrin association with membrane order.

2.4 Discussion

In this study, membrane order within β1 integrin adhesive complexes was examined in cultured primary mouse embryonic fibroblasts and metastatic breast cancer epithelial cells. The study captured β1 integrin's membrane phase preference throughout the life cycle of integrin-mediated adhesive complexes, from early stages of cell spreading to later stages of immobility, by fixing cells after adhering to fibronectin for one hour and 24 hours. Through super-resolution fluorescence localization microscopy, integrins were imaged simultaneously with membrane markers that have previously shown a lipid phase preference. The high resolution of the imaging (~25nm) partnered with cross-correlation analysis allows the visualization of weak enrichment or depletion of the membrane probes surrounding β1 integrins.

The total β1 integrin populations, i.e., integrins in all conformational states, were imaged simultaneously with peptides that sort into different regions of membrane order. The results conclude that during cell spreading and attachment (1 hour fixation), β1 integrins co-localize with both markers of membrane phase preference. Here, the composition surrounding the β1 integrins more homogeneous, i.e., similar enrichment of both liquid-order and liquid-disorder lipids. This provides evidence that immature β1 integrin containing adhesions are not associated with membrane order.

At 24 hours, both markers continue to be recruited to integrins at short distances, but the extended correlation with the membrane order probe reaches far past the enrichment of the disordered probe. I speculate that the long-tail in the cross-correlation plot represents the long, fibrillar adhesion structure. The density-based algorithm (DBSCAN) is used to assign localizations to clusters and determine how the membrane probes co-localized with adhesive structure. With this analysis, it is evident that order-preferring probes are recruited to adhesions in cells that have attached for 24 hours, but no order preference for cells that have attached for one hour. The structures present at longer attachment times are larger, so it possible that these structures can more easily stabilize a heterogeneous composition. It is also possible that the remodeling of the extracellular matrix affects the integrin conformational state in such a way that it impacts the lipid composition.

In the metastatic breast cancer cell line, MDA-MB-231, active conformation of β1 integrins, which are isolated to adhesive complexes, co-localize order preferring probes over disorder-preferring probes. This demonstrates that in at least this cell line, the active conformational state of β1 integrins co-localize with membrane-order preferring probes. In general, active conformer β1 integrins are correlated with adhesions only, so these data also support the hypothesis that

adhesive complexes are regions of membrane order. It is interesting that the β1 integrins in the MDA-MB-231 cell line are correlated with the marker of membrane order and not the liquid-disorder probe as the MEF cells are. This might be a characteristic of the pathology of the MDA-MD-231 cells and may be linked to the previous reports indicating this cell line has a distinct cellular lipid profile that correlates with its metastatic potential [20, 110, 126, 128].

Computing the cross-correlation locally, instead of across the whole membrane area, highlights that averaging over large areas particularly impacts this system. This is due to the heterogeneity of structure and subcellular location of adhesions between cells imaged from the same dish. It also allows to cut out long-scale artifacts contributed to an uneven distribution of adhesions across the cell membrane or membrane topology that leaves holes in the reconstructed images. Both methods are in general agreement with each other, showing an enrichment of membrane order preferring peptides correlating with the structure of the mature, fibrillar adhesions present at 24hr attachment.

In summary, this Chapter examined the spatial distribution of lipids in β1 integrin-mediated adhesion across two cell lines. In both types of cells, β1 integrin-containing adhesive complexes are regions of membrane order through computed cross-correlations of the localizations from reconstructed images. Further work will need to be done to determine if there is a dependence on integrin conformational state to membrane order (discussed in Chapter 3), or how membrane composition perturbations affect the signaling cascade downstream of integrins, such as Src family kinases, Ras, Rac1, or RhoA [96, 100]. Additionally, it will be essential to characterize further the spatial distribution of lipids surrounding other integrins, such as β3 mediated adhesion, because reports have indicated they have different roles in adhesion and migration [129].

2.5 Materials and Methods

2.5.1 Cells and transfection

Non-inbred mouse strain, Primary Mouse Embryonic Fibroblasts (MEFs) were purchased from the American Type Culture Collection (ATCC, cat # SCRC-1040). MEF cells were maintained in Dulbecco's Modified Eagle's Medium (DMEM) modified to contain 4mM L-glutamine, 4500mg/L glucose, 1mM sodium pyruvate, and 1500mg/L sodium bicarbonate (Gibco, Thermofisher Scientific, Waltham, MA), 15% heat-inactivated, fetal bovine serum (FBS) (Mediatech Corning, Manassas, VA catalog#35-011-CV) , and 100 U/mL Penicillin-Streptomycin (ThermoFisher Scientific) in 5% CO_2 at 37°C. Only low passage (two through seven) were used for experimentation. MEF cells were transiently transfected used a Lonza 4D Nucleofector electroporation system (Lonza, Basel, Switzerland), P4 Primary Cell X Kit S (Lonza, Catalog# V4XP-4032). Plasmid DNA encoding for PM-mEos3.2or TM-mEos3.2 was used for transfection. For each transfection, 100,000 cells were electroporated using 16.3uL P4 nucleofector solution, 3.6uL of P4 supplement, and 2ug/mL of each plasmid. Following electroporation, cells were in a sterile culture hood for 10 minutes, then 80uL of CO_2 full MEF culture media was pipetted into the nucleocuvette. Cells were then placed in the incubator in the nucleocuvette to continue to recover for 10 minutes. Following transfection, cells to be used in 1hr attachment experiments were diluted into 200ul full MEF media, and 100uL aliquots were placed into a 12 well microplate containing 1mL CO_2 equilibrated MEF media. For 24hr attachment studies, cells were diluted into 300uL media, and 100uL of cells was subsequently plated directly onto fibronectin-coated dishes MatTek dishes to express overnight.

MDA-MB-231 metastatic breast cancer cell line was a generous gift from Prof. Allen Liu, University of Michigan. MDA-MB-231 cells were maintained in Roswell Park Memorial Institute

(RPMI) medium 1640 1X with L- glutamine to contain 25mM HEPES (Gibco, Thermofisher Scientific, Waltham, MA), 10% heat-inactivated fetal bovine serum (FBS) (Mediatech Corning, Manassas, VA catalog#35-011-CV) , 5μg/mL Gentamicin (Gibco, Thermofisher Scientific), and 100 U/mL Penicillin-Streptomycin (ThermoFisher Scientific) in 5% CO_2 at 37°C. MDA- MB-231 cells were transiently transfected using were transiently transfected using a Lonza 4D Nucleofector electroporation system (Lonza, Basel, Switzerland), SE Cell X Kit S (Lonza, Catalog# V4XC-1032). Plasmid DNA encoding for PM-mEos3.2or TM-mEos3.2 was used for transfection. For each transfection, 100,000 cells were electroporated using 16.3uL SE nucleofector solution, 3.6uL of SE supplement, and 2ug/mL of each plasmid using pulse code #CH-125. Following electroporation, cells were in a sterile culture hood for 10 minutes, then 80uL of CO_2 full MDA-MB-231 culture media was pipetted into the nucleocuvette. Cells were then placed in the incubator in the nucleocuvette to continue to recover for 10 minutes. Following transfection, cells to be used in 1hr attachment experiments were diluted into 200ul full MDA-MB-231 media, and 100uL aliquots were placed into a 12 well microplate containing 1mL CO_2 equilibrated MDA-MB-231 media. For 24hr attachment studies, cells were diluted into 300uL media, and 100uL of cells was subsequently plated directly onto fibronectin-coated dishes MatTek dishes to express overnight.

2.5.2 Cell plating and dish coating

Cells were plated on 35mm, No. 1.5 coverslip dishes with 14mm glass diameter (MatTek, Ashland, MA Catalog #P35G-1.5-14-C). Before plating dishes were plasma cleaned (Harrick Plasma, Ithaca, NY. Model# PFCDC-32G). Dishes were immediately coated with 100uL (0.01mg/mL) fibronectin from human plasma (Millipore Sigma, St. Louis, MO, cat# F2006) and placed in a 5% CO_2 at 37°C incubator for 1hr. Dishes were rinsed with warm, sterile 1X phosphate

buffered saline (diluted from 10X stock, Gibco, ThermoFisher Scientific). For 1hr attachment experiments, cells expressing membrane anchor plasmids were trypsinized from their microplates, spun at 90xg for ten minutes, and plated directly onto the glass well of the MatTek dishes in full media and moved to the 5% CO_2 at 37°C for the hour.

2.5.3 Fixation and labeling for super-resolution imaging

Following the wash, cells were blocked in 10% goat serum for 1hr at room temperature. β1 integrin activation state then was labeled through a primary and secondary antibody labeling scheme. Total β1 integrin population in MEF cells was labeled through rat anti-mouse antibody, clone MB1.2 (EMD Millipore, cat #MAB1997), diluted 1:100 in 10% goat serum at room temperature for one hour. Activation conformers of β1 integrins in MEF cells were labeled with rat anti-mouse antibody, clone 9EG7 (BD Bioscience, cat#553715), diluted 1:100 in 10% goat serum at room temperature for one hour. Activation specific conformers of β1 integrins in MDA-MB-231 cells were labeled with the mouse anti-human monoclonal antibody, clone #12G10 (Millipore Sigma, cat# MAB2247). Following primary antibody labeling, cells were washed three times in 10% goat serum and proceeded to secondary antibody labeling. Total or activation specific integrins antibodies in MEF cells were detected through an AffiniPure goat anti-rat IgG (H+L) antibody (minimal cross-reaction to human, bovine, horse, mouse, and rabbit serum) (Jackson ImmunoResearch, West Grove, PA, catalog# 112-005-167) conjugated to an ATTO-655 fluorophore, diluted 1:100 in 10% goat serum at room temperature for one hour. Activation specific integrins in MDA-MB-231 cells were detected through an AffiniPure goat anti-rat IgG (H+L) antibody (minimal cross-reaction to human, bovine, horse, mouse, and rabbit serum) (Jackson ImmunoResearch, West Grove, PA, catalog# 112-005-167) conjugated to an ATTO-655

fluorophore, diluted 1:100 in 10% goat serum at room temperature for one hour. Finally, cells were washed three times with 10% goat serum and stored 5% goat serum, 0.02% sodium azide solution at 4°C before imaging.

2.5.4 IgG Antibody conjugation to ATTO 655

Goat anti-rat IgG antibody (Jackson ImmunoResearch, catalog# 112-005-167) was modified with ATTO-655 N-hydroxysuccinimide (NHS) ester (Millipore Sigma, cat#76245-1MG-F). 1.3mg of IgG antibody reacted with the ATTO-655 NHS ester in an aqueous solution buffered by 0.01M NaH_2PO_4 pH9.0 with 0.01M NaH_2CO_3 with 65uM of free ATTO-655 NHS ester and 6.5uM IgG antibody at pH8.2 for one hour, protected from light, under gentle agitation using a carousel tube rotator. The reaction was then separated by gel filtration on Illustra NAP-5 Sephadex G-25 columns (GE Healthcare, Piscataway, and New Jersey, catalog #17-0853-02) to separate labeled antibody from unbound dye. Labeled antibody was then spun down at 20,000xg for 90 minutes at 4°C and supernatant removed to separate out protein aggregates. The dye/protein ratio was determined to be 1.6, from absorbance measurements utilizing a NanoDrop 2000 (ThermoFisher Scientific).

2.5.5 Imaging setup and data collection

Total internal reflection fluorescence (TIRF) microscopy was achieved using an Olympus inverted microscope (model # IX81-XDC), accompanying cellTIRF module, and a 100X UAPO TIRF objective (NA=1.49) (Olympus America). Excitation of ATTO-655 was accomplished using a 647nM diode laser (OBIS 647 LX-100FP, Coherent, Santa Clara, CA). Photoactivation of PM-mEos3.2 or TM-mEos3.2 was accomplished with a 405nm diode laser (CUBE 406-50FP,

Coherent). Excitation of PM-mEos3.2 or TM-mEos3.2 was accomplished using 561nm diode laser (Sapphire 561 LP, Coherent or OBIS 561LS 120mW, Coherent). Excitation and emission of mEos3.2 and ATTO-655 dye pairs were filtered using the quadband cube ET-405/488/651/647 (Chroma, Bellows Falls, VT). Emission was split into two separate channels using a DV2 multichannel imaging system (Photometrics, Tucson, AZ) using a T640lpxr dichroic mirror (Chroma) to divide emission. Additionally, ET605/52m filtered near-red emission and ET700/75m filtered far-red emission (Chroma). Individual cells were imaged at low power to capture diffraction-limited TIRF images of clustered β1 integrin and interference reflection microscopy. Images were captured using an iXon-897 EMCCD camera (Andor, South Windsor, CT).

Super-resolution experiments took place under TIRF illumination, adjusted for photoswitching to occur, and single fluorescent events were separated enough to resolve individual events correctly. Cells were imaged in oxygen-scavenging and reducing buffer containing 50mM Tris, 550mM glucose, 10mM NaCl, 12mM glutathione, 40μg/mL catalase from bovine liver (Millipore Sigma, catalog# G7141), and 500 μg/mL glucose oxidase from *Aspergillus niger* type X-S (Millipore Sigma, catalog # G7141) pH 8.5. For each cell, 10-50 movies were collected using custom image acquisition software written by Prof. Sarah Veatch, using MatLab (Mathworks, Natick, MA). Each movie contained 500 images at an integration time of 10-20ms. The entire camera field of view was used during imaging to capture the largest area of the cell as possible.

2.5.6 Super-resolution image reconstruction and single molecule analysis

Raw images of captured single molecule events (stochastically blinking diffraction-limited spots) were background subtracted; then events were localized by fitting local maxima to a two-dimensional Gaussian function. Depending on localization sampling of the cell, reconstructed

images were created from 5,000 to 1.25 x10^6 frames of raw data. All the remaining localized points were then used to form reconstructed images [112]. Localized events that were outliers in brightness, aspect ratio, and spot width were culled based on a user-defined threshold and were not included in the reconstructed image. Additionally, localized events that remained "on" for consecutive frames in a row were counted as one, and every 250 or 500 frames were corrected for stage drift.

Localized events from the near-red emission and far-red emission were registered using 0.1μm fluorescent microspheres in both channels as fiducial markers (TetraSpeck, ThermoFisher Scientific, catalog #T7279). Diluted 0.1μm microspheres (typically 1: 200μL in 1X PBS) were placed on a plasma cleaned MatTek well. The microspheres were then imaged by exciting with both the 561nm and 647nm lasers, and 50-100 images were collected of both channels. Microsphere images were collected at the beginning and end of the movies used to create a super-resolution reconstructed image for a single cell. In order to register the two channels, the images from fluorescent microsphere were used as control points to generate a polynomial transform. The polynomial transform was then applied to the near-red emission channel for image reconstruction. Finally, the reconstructed images event localization precision or resolution was calculated from correlation function analysis [130] and were routinely approximately 25 to 30nm.

2.5.7 Correlation function analysis of reconstructed images

The cross-correlation of reconstructed images from super-resolution experiments to quantify the co-localization of two distinct fluorophores (corresponding to a lipid-phase marker and an integrin) in fixed cells [112]. The cross-correlation function, C(r), measures the probability of finding a pair of two unique fluorophores in the same vicinity as a function of their distance, r.

In general, the process to determine the cross-correlation on reconstructed images begins with defining the region of interest to calculate the cross-correlation. This is accomplished by masking the cell or region of interest, discounting cell edges or regions sharp membrane protrusions. Within the mask area all the pairwise distances between the all the localizations are tabulated and a histogram, H(r), is generated. The bins of the histogram are centered on r, and the bin size is Δr. This is analogous to a circular area core of radius r, and Δr as a shell of area surrounding the core. With each additional bin, another shell of area of Δr is added on, the area of each shell or bin is represented by $\Delta A_{bin}(r) = 2\pi\Delta r$. As the bin size increases, there is an increased likelihood that pairs that are randomly distributed are separated a large distance. To correct for this, H(r) is normalized to a histogram of randomly distributed localizations across the same area, N(r). The cross-correlation of the unique pairs is expressed as Equation 1.

$$\boldsymbol{C(r) = \frac{H(r)}{N(r)}}$$

Equation 1: Cross-correlation of unique probe pairs

The size of the dataset from a single reconstructed image is very large, so to reduce the calculation load the cross-correlation function is tabulated using fast Fourier transforms (FFTs) [130]. In this method, two reconstructed images from the far-red emission channel (I_1), the near-red emission channel (I_2), and their respected average localization densities, ρ_1 and ρ_2, and the applied mask (M) are used to calculate C(r) according to Equation 2.

$$C(r) = Re\left\{\frac{FFT^{-1}(FFT(I_1) \times conj[FFT(I_2)])}{\rho_1\rho_2 \times FFT^{-1}(|FFT(M)|^2)}\right\}$$

Equation 2: Cross-correlation tabulated using fast Fourier transforms

where *conj* [ ] indicates the complex conjugate and Re { } indicates the real part. As shown previously [130] the correlation function calculated using the FFT method returns the same results as the cross-correlation was calculated manually.

2.5.8 Density-based clustering analysis

To delineate between clusters found in adhesion and non-adhesion structures, the Density-Based Spatial Clustering of Applications with Noise (DBSCAN) algorithm is applied to reconstructed images [123, 124]. DBSCAN operates by counting the number of points in a user-defined radius and applying a minimum point threshold to identify core, border, and noise points. In this study, the radius was set to 100nm, with a minimum point threshold of ten per cluster.

Core points are in the interior of the cluster radius and its included neighbors within the radius surpass the minimum threshold point. Border points are defined as a point that is within the radius but does have enough neighbors to pass the minimum threshold. A noise point is any point that is neither a core or border point. Using this information DBSCAN segments the data points into clusters. DBSCAN must calculate the distance between each neighboring point, so the runtime of DBSCAN scales with the size of the whole dataset squared. To combat long runtimes, the image is divided into a grid and DBSCAN runs across smaller areas. Consequently, the grid crosses over adhesion structures; incorrectly identifying one adhesion as two separate structures. To resolve this artifact issue, DBSCAN is run twice.

In the second pass through DBSCAN, the grid is shifted to the right, and data sets merged so contiguous structures can be identified. This modified DBSCAN algorithm readily identifies integrins clustered to form adhesions and those outside adhesions.

The spread of localizations assigned to an adhesion is plaque-like in appearance and the spread out diagonally. When spread diagonally, the overall shape of the data is defined by the covariance matrix, whereas the variance defines axis-aligned spread. From this the eigenvalue of the covariance matrix is calculated to determine the length of the adhesion along the long and short axes. To be considered a clustered adhesion, the long axis must be greater than 1μm.

Chapter 3: The Conformational State of β1 Integrins does not Contribute to Membrane Order in Adhesions but is Sensitive to Membrane Perturbations

3.1 Chapter Overview

In Chapter 2, I determined that β1 integrins associate with both markers of membrane order and disorder, but found that clustered integrins found in adhesions prefer membrane order. This result motivates an examination of how active conformation β1 integrins associate with markers of membrane order. In this Chapter, I determine that the active conformation β1 integrins, which are confined to adhesions, do not exhibit a stronger preference for an ordered membrane environment in mouse embryonic fibroblasts versus the total population of integrins. I also examine how the active conformation of integrins is distributed across adhesive complexes, and find that adhesions are made up of integrins in at least two different conformational states. Finally, I show that exposure of cells to *n*-alcohols, which perturb membrane composition in the plasma membrane, bias the activation state of integrins.

3.2 Introduction

Adhesive complexes are sites of integrin extension, and evidence indicates that both external ligand and cytoplasmic binding partners stabilize an extended conformation found in adhesive complexes [2, 131, 132]. As a result, the extended active conformation of the integrin receptor is hypothesized to carry out integrin signaling and drive integrin oligomerization. Integrin activation is fully discussed in Chapter 1. In brief, integrins exist in different conformational states that are used to specify their activation state or affinity for ligand [1, 19, 21-23, 26, 133-136]. The current

model for integrin activation has integrins adopting at least three different conformational states that relate to our understanding of activation. In general, a global conformational change from "bent" receptor to "upright-extended" receptor is accepted as required for integrin activation [4, 137-139]. Intermediate conformational states also exist, which occur when the integrin is partially bent [25], upright-extended without an open headpiece available for the ligand, or extended with fused transmembrane sequences [132]. However, the subcellular locations of different conformations, if intermediate conformations elicit a cellular response, and if all 24 mammalian heterodimeric integrin pairs adopt the same conformational changes remains controversial [140].

Extensive structural studies on integrins have revealed numerous ways to bias integrin activation including varying ligands [141], divalent cations [27], disulfide bond reduction [142], and stimulatory or inhibitory monoclonal antibodies [24]. Evidence indicates that membrane compositions can alter cellular adhesion or integrins themselves. In one study, cholesterol depletion was shown to decrease cell adhesion in cells, despite being in the presence of an excess of the multivalent ligand, fibronectin [85]. In the same study, perturbing plasma membrane cholesterol content was shown to affect the actin-cytoskeleton network and the phosphorylation of two signaling molecules downstream of integrins – focal adhesion kinase (FAK) and p44/42 mitogen-activation protein (MAP) kinase. In the present study, membrane perturbations are introduced through the use of long-chain *n*-alcohols. Long-chain *n*-alcohols are amphiphilic, meaning they have polar and non-polar ends, which allow them to permeate or intercalate the membrane. The *n*-alcohols used in this study have previously shown to impact the physical properties of giant plasma membrane vesicles (GPMVs) [143, 144] and are hypothesized to impact regions of membrane order intact cells.

In Chapter 2, I concluded that β1 integrin containing adhesive complexes are regions of membrane order, and I hypothesize that the conformational state of the integrin dictates this environment. To explore this hypothesis, I first use conformational specific antibodies to characterize the relationship between active integrins and markers membrane composition through dual color super-resolution localization microscopy. Total internal fluorescence microscopy (TIRFM) combined with interference reflection microscopy (IRM) is used to visualize the subcellular locations of the active conformation of integrins as it relates to the adhesive complexes. Finally, I demonstrate that the addition of membrane intercalating long-chain *n*-alcohols can bias integrin activation state, providing further evidence that β1-containing adhesive complexes - or the regulatory network that governs them - is sensitive to membrane composition.

3.3 Results

3.3.1 Adhesions are heterogeneous complexes of integrins in different conformations

Figure 3-1 shows a representative image of a cellular footprint obtained through interference reflection microscopy (IRM). The grey shadows signal represents where the cell is attached to the glass. Through a combination of both interference reflection microscopy and immunofluorescence, I determined that adhesive complexes are heterogeneous complexes of at least two different conformations of β1 integrins. In Figure 3-2, The monoclonal antibody, clone 9EG7, recognizes explicitly β1 integrins that are in an active conformation, i.e., an upright and extended with separation between the cytoplasmic tails of the α and β integrin subunits [1, 2, 132, 145]. The monoclonal antibody, clone 1997, detects total β1 integrin content.

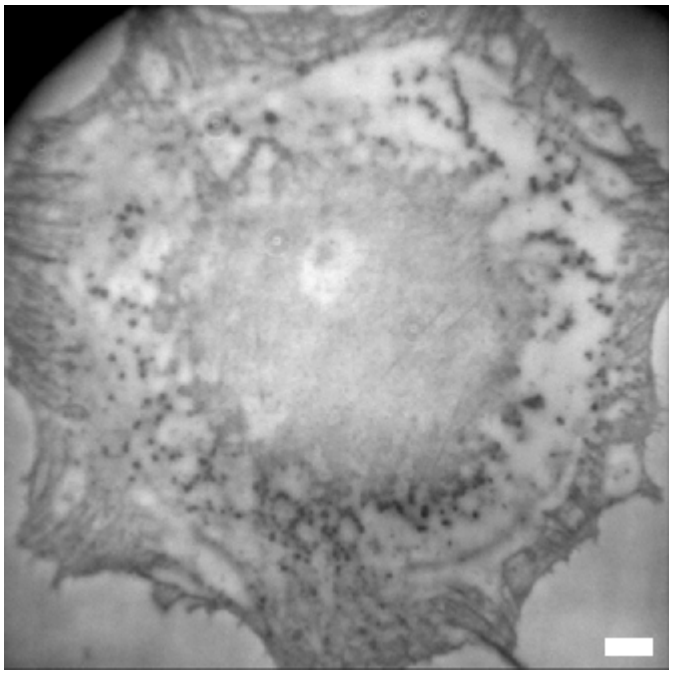

Figure 3-1 Interference reflection microscopy outlines the cellular footprint

Representative image of a cellular footprint obtained through interference reflection microscopy (IRM). The grey shadows signal represents where the cell is attached to the glass. Scale bar is 5μm.

In Figure 3-2, the black and grey shadows represent a cellular footprint of what is attached to the glass; the pure red background indicates sites of no adhesion. The green signal represents the antibody label. In Figure 3-2, panel A, the total β1 integrin label co-localizes with all areas of cellular contact with the glass, both inside and outside adhesives complexes at 1hr. In contrast, at the same time point the active conformer label is isolated to adhesive complexes (Figure 3-2, panel B), and only represents a portion of the complex. This is indicated by the long, black stretches in the interference contrast microscopy image in between the green patches that represent the active conformer. At 24-hour attachment, total integrins remain co-localized with all areas of cellular contact, as shown in Figure 3-2, panel C. The adhesive complexes remain segmented with active

conformer integrins even at 24-hour attachment, as shown in Figure 3-2, panel D. The active conformer takes up even less area in adhesive complexes found at 24-hour attachment.

In Figure 3-3, panels C and D from Figure 3-2 are magnified to emphasize how the adhesions are segmented. The white arrows on Figure 3-3, panel D indicate a representative site where total β1 integrin would label the adhesion, indicating the location where intermediate stage exists. Together, these data show that β1 integrin containing adhesive complexes are made of up integrins in at least two different conformational states, and only contain only a subset of integrins hypothesized to be responsible for integrin signaling and function.

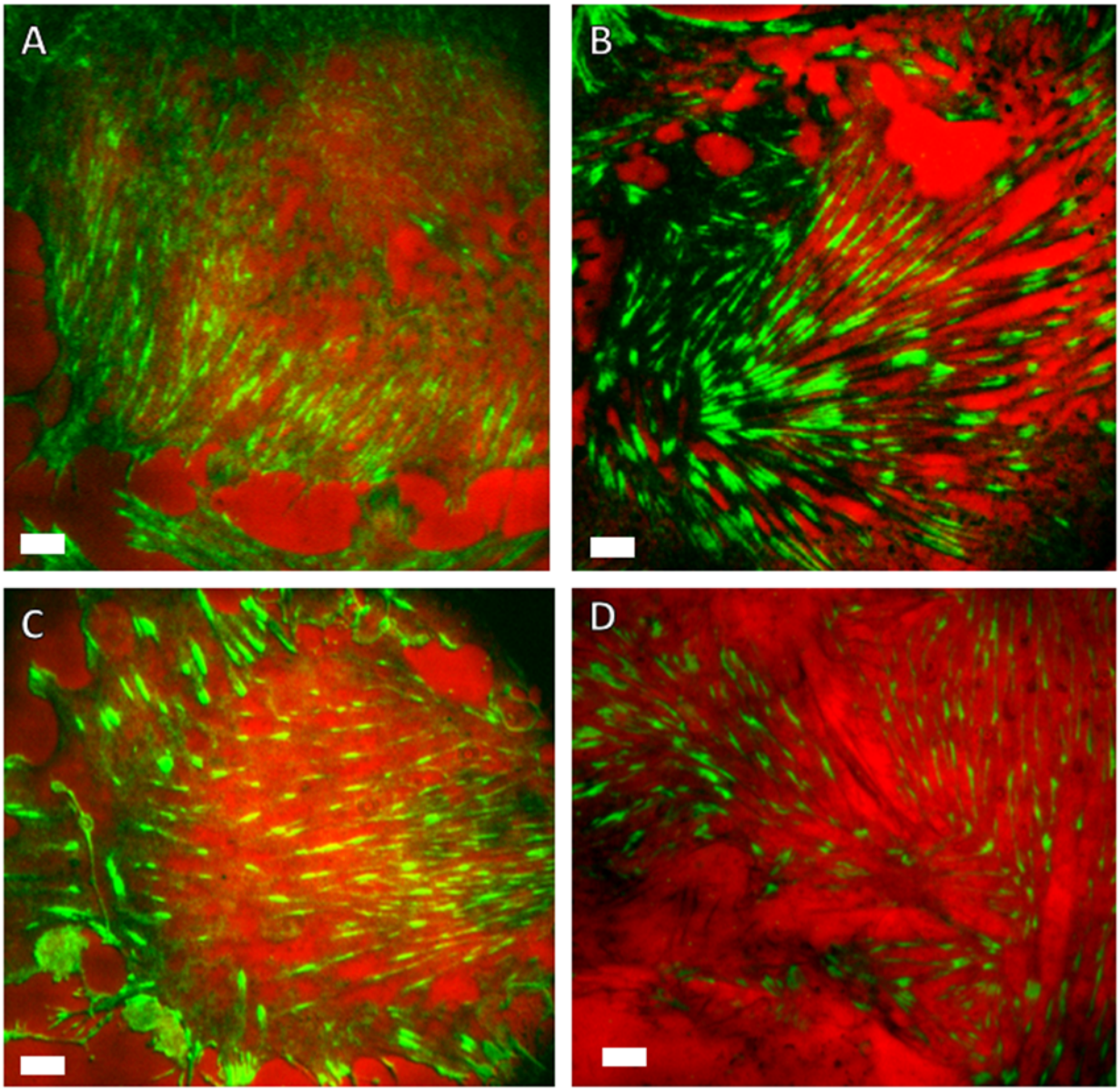

Figure 3-2: MEF Adhesions are heterogeneous complexes of β1 integrins in different conformations

Interference reflection microscopy images (black, grey and red background) and total internal reflection fluorescence microscopy images β1 integrin (green) are merged to demonstrate conformational heterogeneity in β1 mediated cellular adhesion. MEF Cells adhered to fibronectin for 1hr or 24hrs. Scale bars 5μm. A) Total β1 integrin at 1hr B) Active conformation β1 antibody at 1hr C) Total β1 integrins content at 24 hours. D) Active conformation β1 antibody at 24hr.

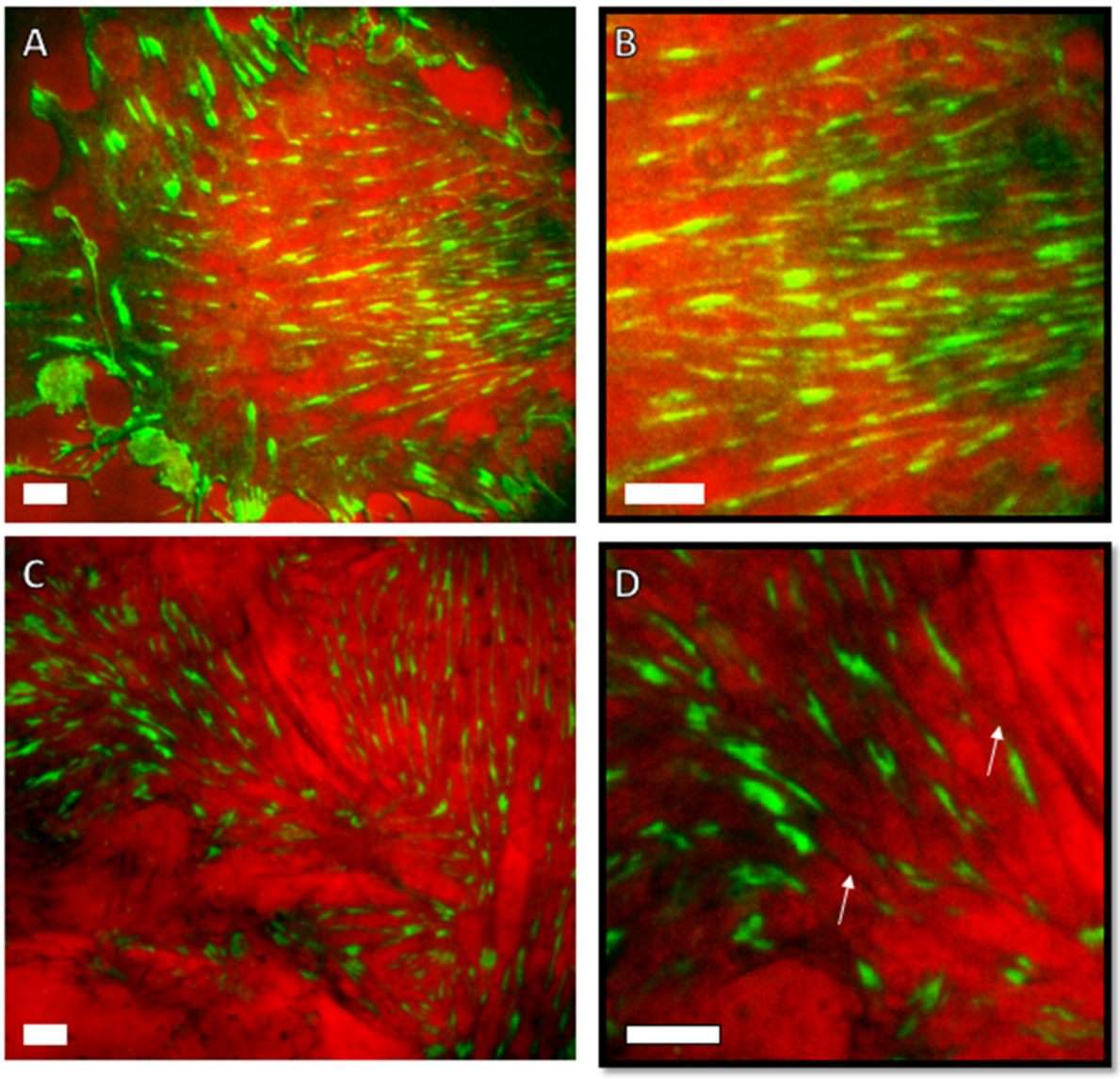

Figure 3-3: MEF Adhesions are heterogeneous complexes of β1 integrins in different conformations (magnified)

Interference reflection microscopy images (black, grey and red background) and total internal reflection fluorescence microscopy images β1 integrin (green) are merged to demonstrate conformational heterogeneity in β1 mediated cellular adhesion. MEF Cells adhered to fibronectin for 1hr or 24hrs. Scale bars 5μm. A) Total β1 integrin at 24-hour attachment B) Magnified region of panel A demonstrates adhesions are filled in C) Active conformation β1 integrins at 24 attachment D) Magnified region of panel C, demonstrates regions of different β1 integrin conformational state.

3.3.2 Phosphotyrosine co-localizes with only a subset of active conformation integrins

Integrin signaling activity was probed through antibody detection of non-receptor or protein specific phosphotyrosine levels at adhesion sites. β1 integrin cytoplasmic subunits and other enzymatic proteins at adhesion sites are phosphorylated which modulates downstream signaling activity [146]. In Figure 3-4, total internal fluorescence microscopy is used to show where active conformation of β1 integrin receptor (red) and phosphotyrosine levels (green) co-localize (represented in yellow). At one hour attachment, the signaling activity is largely restricted to the cell periphery and protrusions (Figure 3-4 panels A and B). Interestingly, not all active conformers co-localize with phosphotyrosine activity, which indicates active conformation integrins cannot be used as a marker for cell signaling within adhesions. The trend extends to cells fixed at 24-hour attachment, as shown in Figure 3-4 panels C and D.

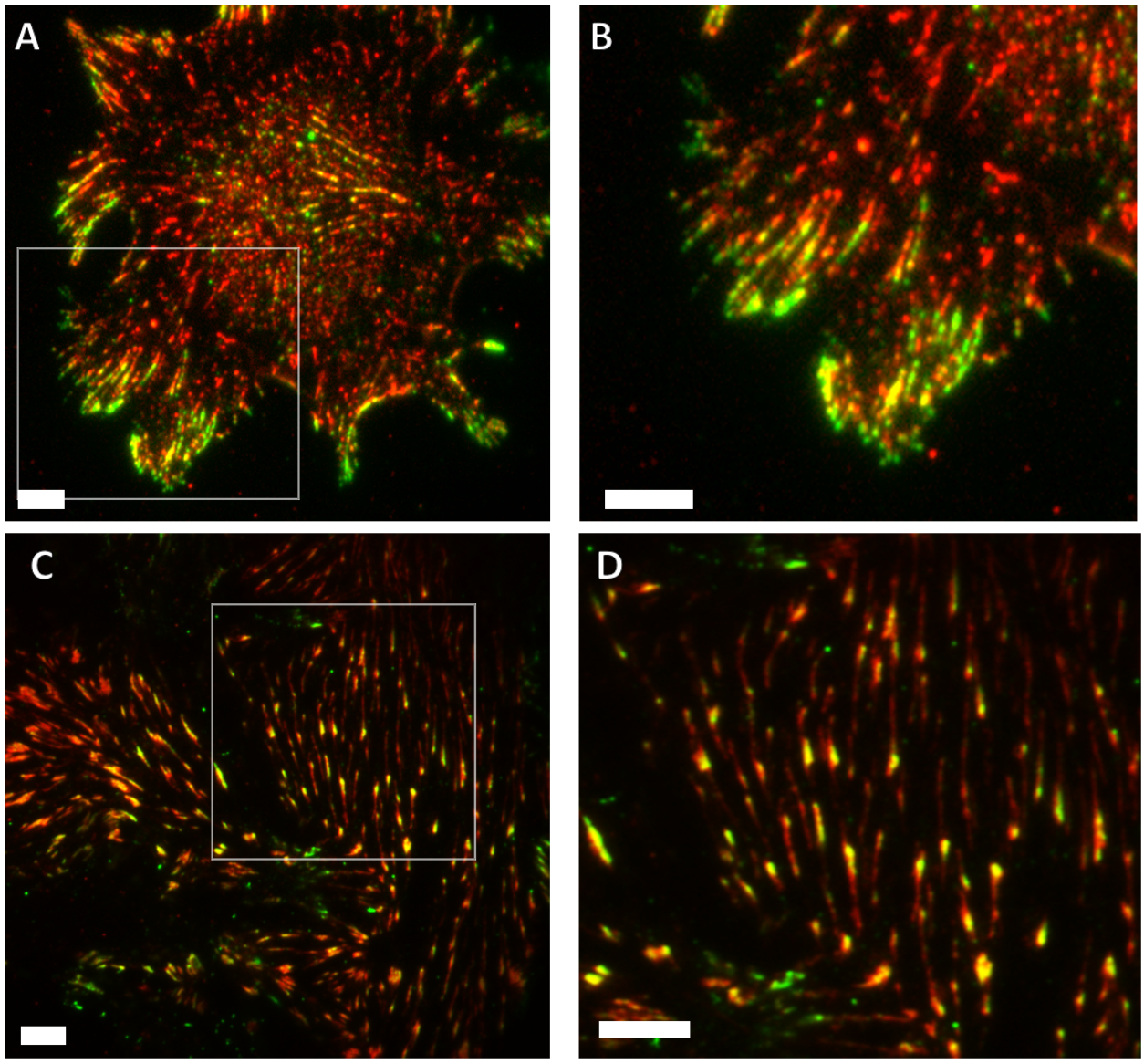

Figure 3-4: Only a subset of active conformation integrins co-localize with phosphotyrosine at 1hr and 24hr attachment

Fluorescent microscopy images of active conformation β1 integrin (red) and phosphotyrosine levels (green) are merged to demonstrate where the most active integrins are located in adhesions. Yellow regions are where the signal overlap. Scale bars are 5μm. A) 1hr attachment B) Magnified region of Panel A, marked with grey box in panel A. C) 24hr attachment D) Magnified region of Panel C, marked with grey box in panel C.

3.3.3 Relationship between conformationally active β1 integrins and membrane order

Membrane heterogeneity surrounding the active-conformation of β1 integrin receptors was monitored through imaging membrane-anchored peptides in primary mouse embryonic fibroblasts (MEFs), the same method used in Chapter 2. In brief, These peptides have previously shown a preference for liquid-ordered or liquid-disordered phases in model membranes, giant plasma membrane vesicles, and ordered and disordered phase-like domains in intact cells [112]. Liquid-order regions were monitored through PM-mEos3.2 and liquid-disorder regions through TM-mEos3.2. Here, I examine whether or not these active integrins have a different membrane phase preference in MEFs. Cells were plated and fixed at one and 24 hours, and active integrins were detected through a conformational specific monoclonal antibody, clone 9EG7. The lateral distribution of both probes was measured through simultaneous stochastic optical reconstruction microscopy (STORM) [103, 104] and photoactivation localization microscopy (PALM) [105, 106], representative images are shown in Figures 3-5 panels A-B and 3-6 panels A-B. Cross-correlation analysis was performed on the localizations from the reconstructed images.

At 1 hour, active β1 integrin conformers are more correlated with PM than TM (on average 15% vs. 10% respectively), as shown in Figure 3-5C. Together, these indicate that the membrane environment surrounding active β1 integrins only slightly favors an ordered environment on average at short distances (less than 100nm), and overall the area remains homogeneous since β1 integrins co-localize similarly with markers of conflicting membrane order preference.

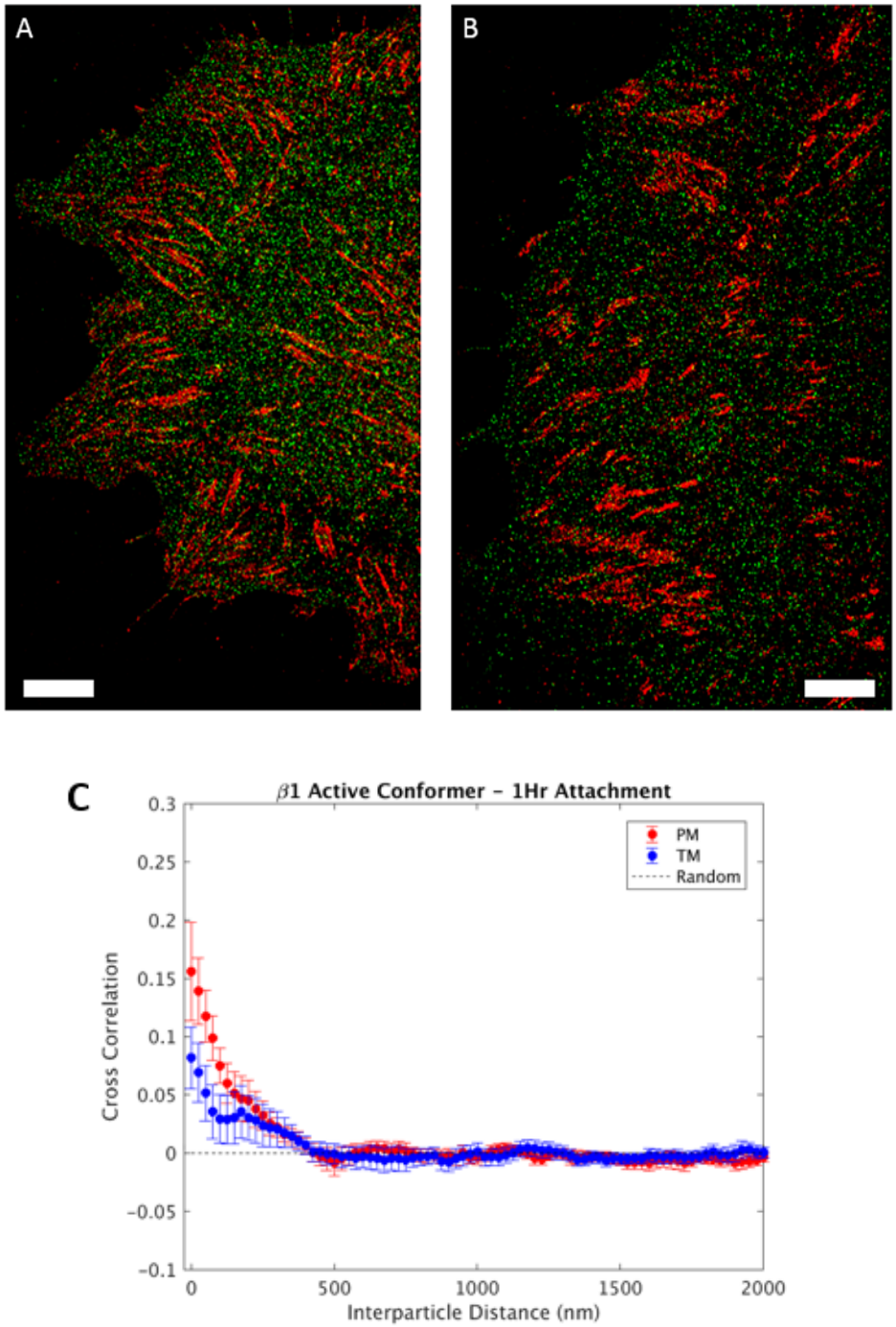

Figure 3-5: Cross-correlation of activation specific β1 integrins in MEFs at 1hr attachment

A) Active conformation β1 integrin conformers (red) and PM (green) membrane probe localization in chemically fixed cells. Scale bar 5μm. B) Active conformation β1 integrin conformers (red) and TM (green) membrane probe. Scale bar 5μm C) The average cross-correlation between of total β1 integrin and PM or TM after adhering to fibronectin for 1 hour. Errorbars reflect the standard error of the mean. 13 cells were imaged and quantified.

At 24 hour attachment, PM and TM are similarly correlated at short distances with the active conformation, under 100nm (Figure 3-6 panel C). There is an emergence of a long tail correlation from 100nm- 1μm, similar to what I reported with the total β1 integrin (Figure 2-2) result. Like in the previous result, I believe the long tail corresponds to the adhesion structure. An examination of active β1 integrins and the membrane order markers reveals that the active conformation only has a slight preference liquid-order like domains, but mostly remains homogenous, i.e., similar enrichment of both markers of membrane order and disorder.

3.3.4 Long-chain n-alcohols bias integrin activation state

Long-chain *n*-alcohols have shown to alter the physical properties of membranes including increasing membrane fluidity, altering membrane transition temperature, decreasing membrane thickness, increasing ion channel transport, and increasing membrane area [147-151]. Here, the effects of two long chain *n*-alcohols, 1-octanol and 1-hexadecanol, are used to modulate the conformational state of β1 integrins. The concentrations of alcohols used in this study were shown to affect the chain melting temperature or phase transition temperature in GPMVs [143, 144, 152]. In intact cells, the *n*-alcohols are predicted to stabilize (1-hexadecanol) or destabilize (1-octanol) ordered and disordered domain structures within the plasma membrane. For example, treatment with 1-octanol is expected to reduce the size and lifetime of phase like domains resident with the plasma membranes of treated cells. Alternately, treatment with 1-hexadecanol is expected to increase the lifetime of phase-like membrane domains.

MEF cells were plated on fibronectin and subjected to an alcohol exchange cation assay as outlined in Materials and Methods. The assay allows the cells to attach in full serum media and then incubate in a minimal media that keeps the integrins engaged with a physiological level of

divalent cations for basal integrin activation without the presence of serum. After the *n*-alcohols permeate the membrane, the effect on the activation state of integrins is assessed through binding of the active conformation-specific antibody to integrins on the cells (primary antibody clone 9EG7 and a secondary antibody conjugated with Alexa Fluor 647). In this assay, cell brightness reports conformationally active integrins on the cell, e.g., brighter the cell, more engaged, conformationally active integrins are present.

The exposure of the cells to the different *n*-alcohol conditions had a strong effect on integrin activation; representative images are shown in Figure 3-7 panels A-C. In Figure 3-7, panel A is the 1% DMSO control (the solvent used to solubilize the *n*-alcohols), panel B is treatment with 1-hexadecanol, and panel C is treatment with 1-octanol. The representative images show an increase in integrin engagement and adhesive complex formation for cells exposed to 1-hexadecanol (Figure 3-7, panel B). Conversely, cells exposed to 1-octanol (Figure 3-7, panel C) show a decrease in overall integrin engagement. The fluorescence intensity data from each *n*-alcohol condition is quantified in Figure 3-7, panel D, normalized to the average cell brightness of the 1% DMSO control. In Figure 3-7, panel D, the 1-hexadecanol fluorescent intensity is 19.1% ± 0.09 greater than the control, and 1-octanol fluorescent intensity is 22.9% ± 0.07 less than the control. Both these values are statistically significant in comparison with the control, 1-hexadecanol has a p-value of 7.6×10^{-4} and 1-octanol a value of 1.3×10^{-6}. In sum, these results show that integrin activation state can be biased changes in membrane composition, likely through the increased or decreased lifetime of the phase-like domains that form on the plasma membrane.

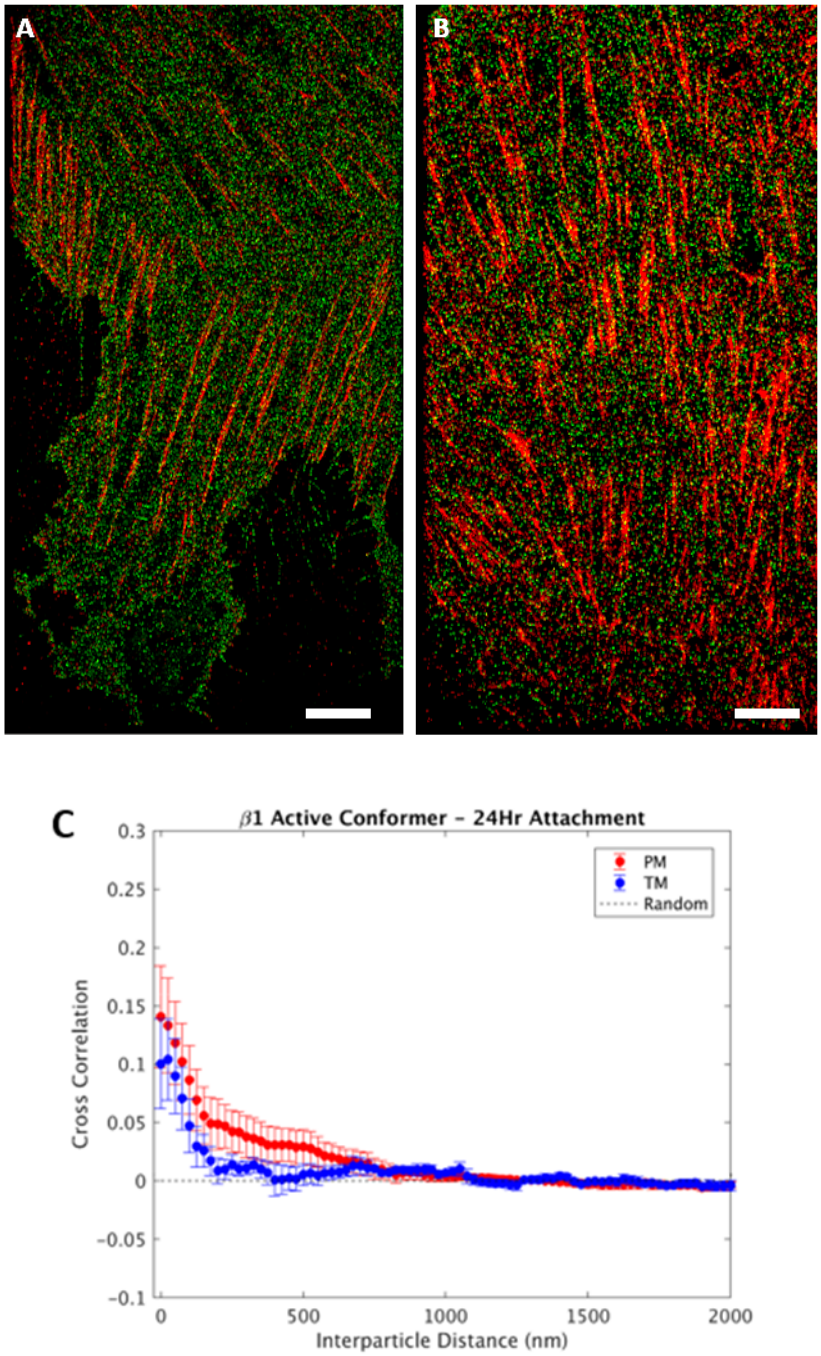

Figure 3-6: Cross-correlation of activation specific β1 integrins in MEFs at 24hr attachment

A) Active conformation β1 integrin conformers (red) and PM (green) membrane probe localization in chemically fixed cells. Scale bar 5μm. B) Active conformation β1 integrin conformers (red) and TM (green) membrane probe. Scale bar 5μm C) The average cross-correlation between of total β1 integrin and PM or TM after adhering to fibronectin for 1 hour. Errorbars reflect the standard error of the mean. 16 cells were imaged and quantified.

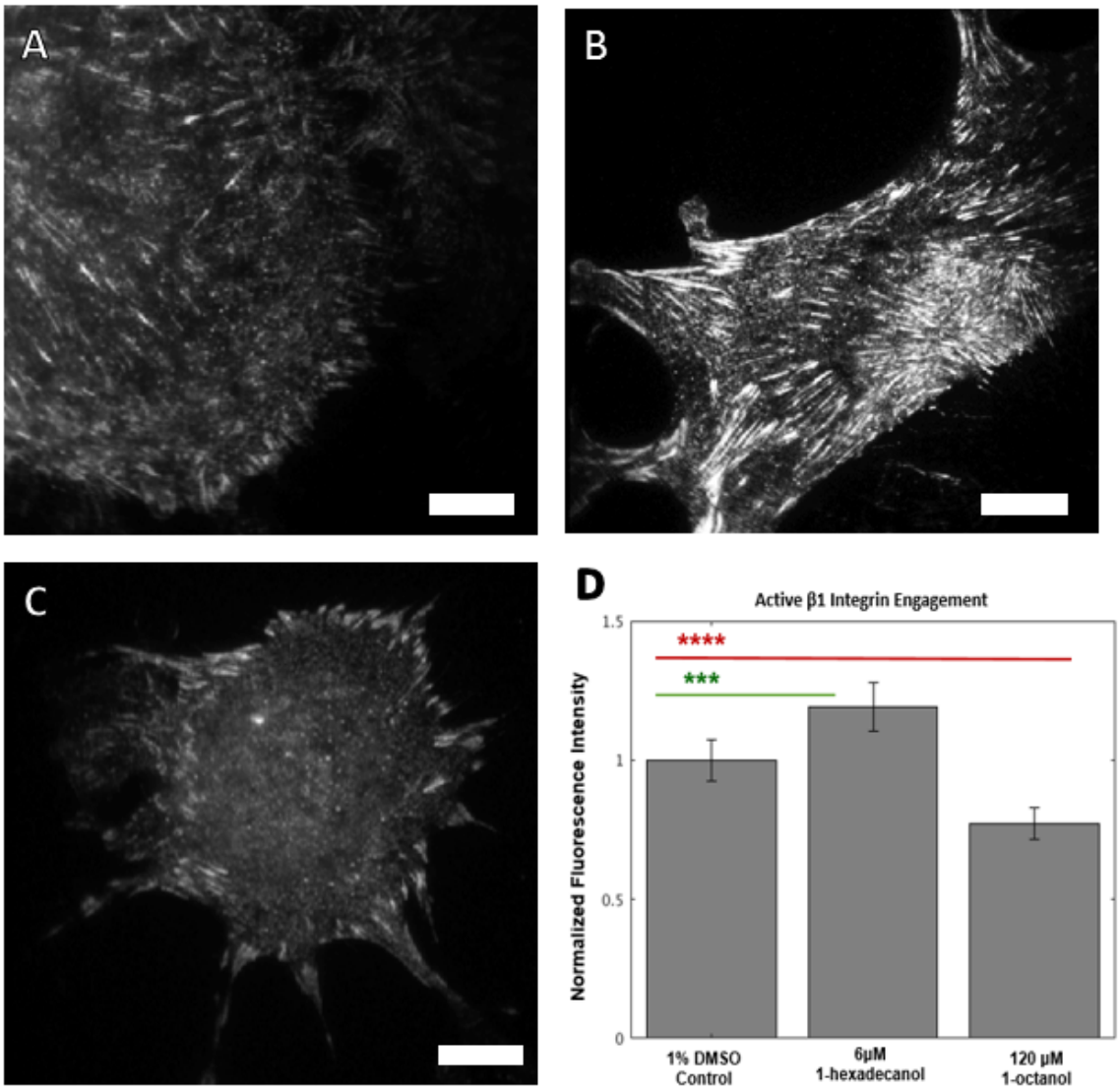

Figure 3-7: Effects of long-chain *n*-alcohols on β1 integrin activation state

Plated cells spread on fibronectin for one hour in full media before being subjected to a modified Tyrode's solution without serum with physiological levels of divalent cations to maintain a basal level of integrin activation. Active conformation integrins were labeled with rat anti-mouse, clone 9EG7 antibody, this was then detected through secondary antibody conjugated with Alex Fluor 647 under TIRF illumination. Long chain alcohols were diluted in 1% DMSO for solubilization purposes. All scale bars are 5μm are on representative images. A) 1% DMSO control B) 6μM 1-hexadecanol C) 120μM 1-octanol D) Bar graph quantifying active β1 integrin engagement through antibody detection after exposure to long-chain *n*-alcohols. Errorbars reflect the propagation of uncertainty taking in account the 1% DMSO control. 63 cells of each condition were imaged and quantified. Panels A – B were rendered with the same contrast and saturation levels. Brightness was normalized across cell area. Asterisks are used to mark statistical significance, *** indicates a $p < 0.001$ of significance, and **** indicates a $p < 0.0001$.

3.4 Discussion

In this study, the subcellular location of active conformation β1 integrins and their relationship with plasma membrane composition was examined in primary mouse embryonic fibroblasts. Through the use of total internal fluorescence microscopy partnered with interference contrast microscopy, I determined that β1 integrin-mediated adhesions are composed of integrins of at least two different conformational states. Due to the excess of ligand and the presence of an adhesion complex, it is likely that the integrins are in a stabilized intermediate conformational state, which is not detectable through antibody clone 9EG7. During characterization of clone 9EG7's binding properties, it was determined that the large ectodomains could block the epitope when bent [132], which might be the case here if the intermediate state is partially bent. I conclude that the subcellular location of active conformation β1 integrins is confined to adhesions, but does not represent the entire adhesion complex.

Through immunofluorescence microscopy, I determined that active conformation β1 integrins are segmented into regions that co-localize with phosphotyrosine and those that do not. Integrins and adhesion-associated enzymes are phosphorylated near the β1 integrin tail, so phosphotyrosine levels are a marker for downstream signaling. These data suggest that integrins detected through clone 9EG7 are not all actively signaling, although they are stabilized in an extended conformation. It has been proposed that some conformationally active integrins are just "primed" for activity, i.e., in a stabilized, ligand bound, extended conformation, but not "active" integrins, i.e., a*ctively* mediating a cellular response [153]. My results are in good agreement with this proposal, and the utilization of active conformation-specific antibodies should be used in conjunction with other cell signaling markers before stating they are *actively* signaling.

The relationship of β1 integrin conformational state with its surrounding membrane composition was determined through super-resolution fluorescence localization microscopy. Despite being isolated to adhesive complexes, active conformation β1 integrins only exhibit a slight preference for membrane order at one-hour attachment and 24-hour attachment (Figure 3-8). At the one hour time point (Figure 3-8, panels A and B), active β1 integrins exhibit a stronger preference for PM at short distances. This may be an indication that during oligomerization or nascent adhesion formation that active β1 integrins prefer an ordered membrane environment to function or mature into larger adhesions. Although active integrins exhibit a slight preference for membrane other, there is still an enrichment of disorder preferring probes around integrins (Figure 3-8, panels C and D). The association with both probes indicate the active conformation state of integrins is not responsible for the membrane ordering characteristics in the adhesions.

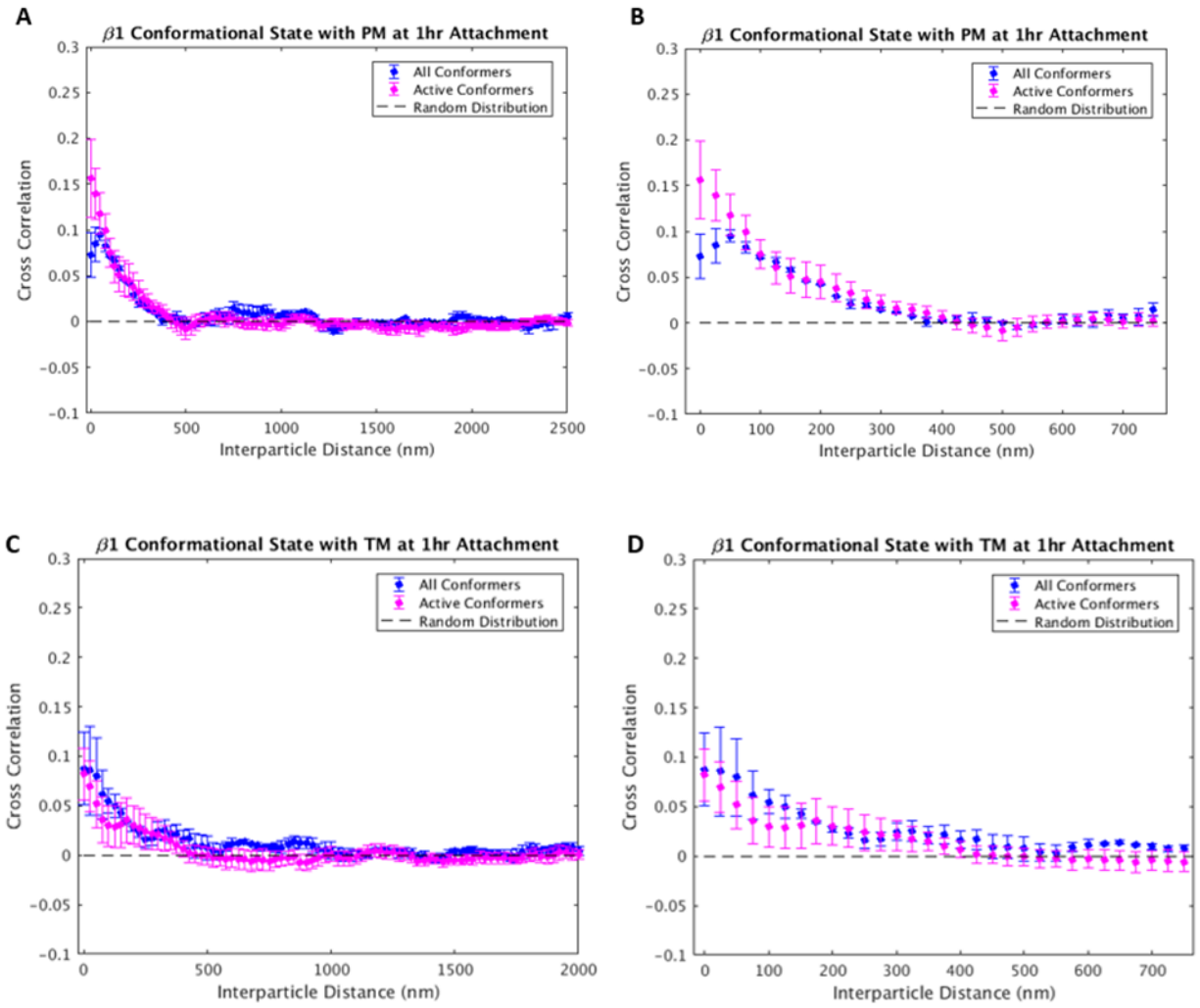

Figure 3-8: Comparison of cross-correlation of all conformational states with membrane markers at 1-hour attachment

The average cross-correlation between of all β1 integrin conformers and PM (Panels A and B) and TM (Panels C and D). Errorbars reflect the standard error of the mean. 13 cells were imaged and quantified for active conformations. Four cells were imaged and quantified for all conformations.

At 24-hour attachment, the membrane environment surrounding active β1 integrins contains both markers of membrane order and disorder, (Figure 3-9) which is demonstrated by the cross-correlations between the active conformation and PM or TM being nearly identical. One feature is distinct, the long-scale correlation present from 100nm-1μm. The emergence of this long-scale correlation was seen in previous experiments (comparison shown in Figure 3-9, panel A), which is representative of the larger adhesion structure. In Figure 3-9, panel A, these data showed an overall decrease in the magnitude of the correlation between active integrins and ordered membrane markers in comparison to the total integrin result. I conclude that active conformation β1 integrins are not the principal mediators of membrane order within adhesions.

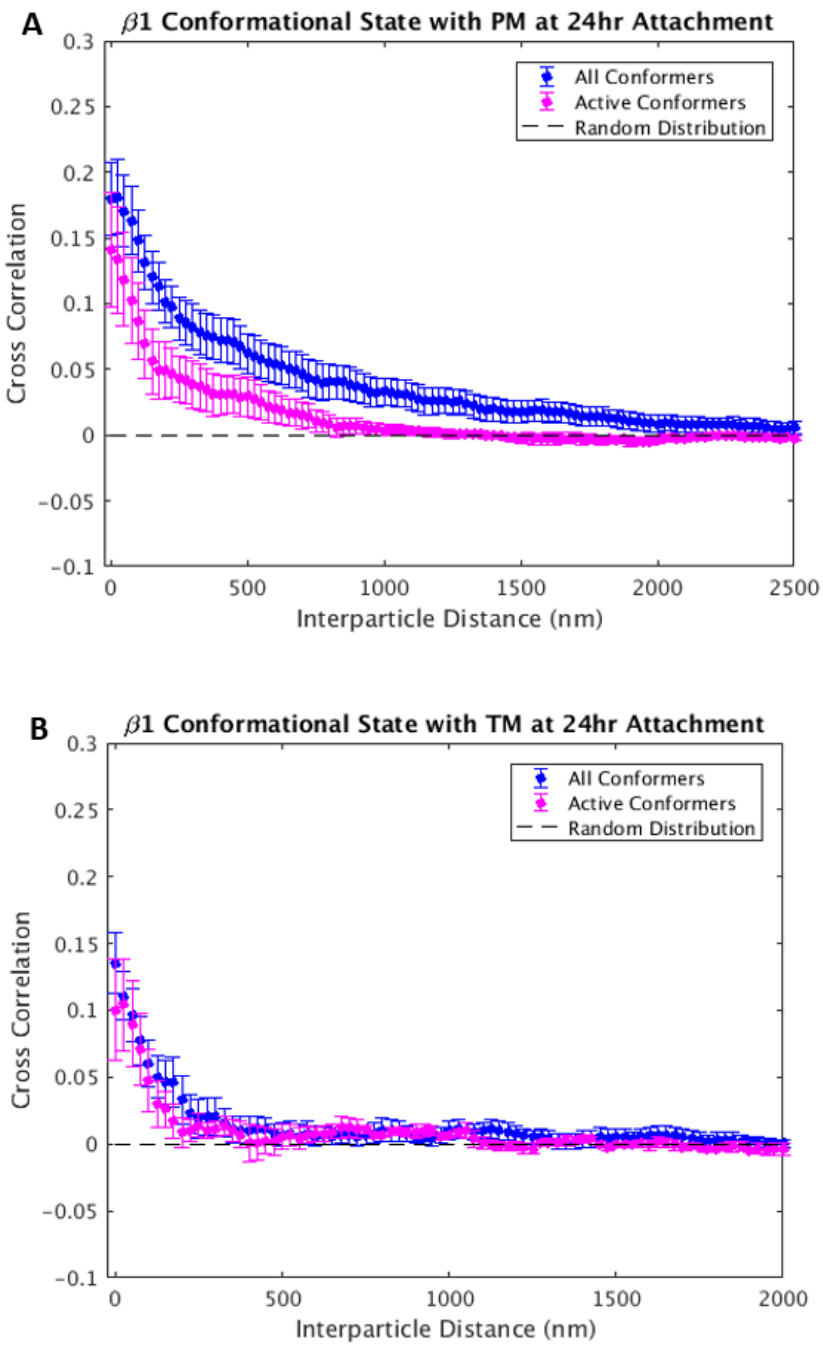

Figure 3-9: Comparison of cross-correlation of all conformational states with membrane markers at 24hour attachment

The average cross-correlation between of all β1 integrin conformers and PM (Panel A, top) or TM (Panel B, Bottom) after adhering to fibronectin for 24 hours. Errorbars reflect the standard error of the mean. 16 cells were imaged and quantified for active conformations. 17 cells were imaged and quantified for all conformations.

Finally, through biochemical compositional membrane perturbations, I found that two long-chain *n*-alcohols are capable of biasing the global conformational changes that occur when integrins activate. 1-Hexadecanol fluorescent intensity is 19.1% ± 0.09 greater than the control, and 1-octanol fluorescent intensity is 22.9% ± 0.07 less than the control. The *n*-alcohols are predicted to increase (1-hexadecanol) or reduce (1-octanol) the size and lifetime of phase-like domains in the plasma membrane of intact cells. This was an interesting result considering I determined that active conformation or total β1 integrins do not strongly associate with membrane order, i.e., the magnitude of the cross-correlation was weaker than predicted and there is an enrichment of peptides associated with disorder. However, there are lipid-dependent "inside-out" pathways for integrin activation. In particular, talin, kindlin, and focal adhesion kinase/Src signaling complex are recruited to β1 integrin tails by interacting through the charged lipid species, phosphatidylinositol 4,5-bisphosphate (PIP2) in the plasma membrane [28, 29, 31-34]. Studies have shown that cell exposure to shorter-chain alcohols reduce PIP2 levels and subsequently suppress PIP2-dependent processes [154, 155]. An analogous interaction might be occurring here, wherein 1-octanol suppresses PIP2 levels preventing the recruitment of the "inside-out" integrin activators, and 1-hexadecanol does the opposite. Further experiments will need to be done to monitor changes in PIP2 levels intact cells before and after incubation with *n*-alcohols, and staining for members of the "inside-out" regulatory network such as talin or the FAK-Src complex.

In summary, experiments and results described in this Chapter determined the subcellular location of active conformation β1 integrins in integrin-mediated adhesion and characterized their association with peptide markers of membrane order. I found that adhesions are heterogeneous complexes of β1 integrins in different conformations and that active conformational state is not

the principal mediator of membrane order that is found in adhesions. Interestingly, integrin activation is modulated through exposure to *n*-alcohols, which I hypothesize is due to altered PIP2 levels and their subsequent impact on recruitment of "inside-out" activators of β1 integrin activation. Further work will need to be done to determine how *n*-alcohols interfere with the "inside-out" activation network of integrins.

3.5 Materials and Methods

3.5.1 Cells and transfection

The cells and transfection materials and procedures used in this study have been outlined previously in Chapter 2, Section 5.1

3.5.2 Cell plating and dish coating

The cell plating and dish coating materials and procedures were outlined previously in Chapter 2, Section 5.2.

3.5.3 Alcohol exchange assay

Plated cells were allowed to attach and spread to fibronectin-coated glass for one hour in full media in 5% CO_2 at 37°C. Subsequently, cells were subjected to a warmed modified Tyrode's solution without serum and physiological levels of relevant integrin-sensitive divalent cations. The modified Tyrode's solution is as follows: 25mM HEPES, 5.6mM glucose, 5mM potassium chloride, 1mM calcium chloride, 1mM magnesium chloride, and 13.5 mM sodium chloride. After 25 minutes, cells were then exposed to a final concentration of 120μM 1-octanol in 1%DMSO and 6μM 1-hexadecanol in 1%DMSO for 30 minutes. Cells were then immediately fixed and labeled for active-conformation β1 integrins using rat anti-mouse antibody, clone 9EG7 (BD Bioscience,

cat#553715), diluted 1:100 in 10% goat serum at room temperature for one hour. The cells were then washed three times in 1X PBS, and active-conformation β1 integrins were detected through a goat anti-rat IgG (H+L) cross-adsorbed secondary antibody conjugated with Alexa Fluor 647 (ThermoFisher, cat #A-21247) diluted 1:100 in 10% goat serum at room temperature for one hour. After three washes with 1X PBS, the actin cytoskeleton was labeled with Alexa Fluor 555 Phalloidin, (ThermoFisher, cat #A-21247) diluted 1:100 in 10% goat serum at room temperature for 30 minutes. Finally, cells were washed three times with 1X PBS, and nuclei were stained with SlowFade Gold Antifade Reagent with DAPI (ThermoFisher, cat# S36938). Cells were then imaged under TIRF illumination, at low laser power. Pixel intensities were then averaged for each cell then normalized by cell area.

3.5.4 Fixation

Cells were washed three times with warm 1X phosphate buffered saline at room temperature. Chemical fixation was completed with 4% paraformaldehyde (Thermofisher Scientific) and 0.01% glutaraldehyde (Ted Pella, Redding, CA) for 10 minutes. Chemical fixation was quenched for five minutes with 10% Goat serum, New Zealand origin (Gibco, ThermoFisher Scientific, catalog#16210072). Cells were then permeabilized for 7 or 15 minutes with 0.1% Triton x-100 (Acros Organics, ThermoFisher Scientific), and washed with phosphate buffered saline three times under gentle agitation.

3.5.5 Antibody labeling for super-resolution imaging

Antibody labeling for super-resolution imaging was described previously in Chapter 2, Section 5.3.

3.5.6 IgG antibody conjugation to ATTO-655

IgG antibody and conjugation to ATTO-655 were described previously in Chapter 2, Section 5.4.

3.5.7 Imaging setup and data collection

Imaging setup and data collection were described previously in Chapter 2, Section 2.5.

3.5.8 Super-resolution image reconstruction and single molecule analysis

Super-resolution image reconstruction and single molecule analysis were described previously in Chapter 2, Section 5.6.

3.5.9 Correlation function analysis of reconstructed images

The cross-correlation analysis of reconstructed images was described previously in Chapter 2, Section 5.7.

Chapter 4: Conclusions and Future Directions

4.1 Overview of Results

Several research groups have reported that integrin-mediated adhesion sites, adhesion-associated enzymes, conformationally active integrins, or integrins in the presence of external ligand have a preference for lipids associated with liquid-ordered membrane domains across several different cell types including fibroblasts, epithelial cells, and lymphocytes [60, 84-89, 94-96, 98-100]. These results support a model wherein extended, conformationally active integrins mediate the association of adhesions sites with membrane order or a liquid-order phase preference through integrin activation.

The experiments and results presented in this dissertation investigated this model to observe how the conformational state of integrins govern its local membrane environment and how and how perturbations affecting lipid composition impact its conformational state. Through super-resolution fluorescence localization microscopy, integrins were simultaneously imaged with membrane markers that have previously shown a lipid phase preference, and their relationship was subsequently quantified. I determined that integrins found within mature, fibrillar adhesions exhibit the strongest preference for membrane order in chemically fixed primary mouse embryonic fibroblasts (MEFs). I found within adhesions; integrins exist in different conformational states and only a subset of integrins in an active conformation co-localize with markers of activity. Furthermore, I determine that active conformation integrins overall do not exhibit a stronger preference for membrane order versus the total integrin population, despite only being localized

to adhesions. Finally, I showed that perturbing membrane composition through incubation with long-chain *n*-alcohols can bias integrin activation and focal adhesion formation. In this Chapter, I will briefly summarize my conclusions and offer suggestions for future work that these data motivate.

4.2 β1 integrin containing fibrillar adhesions are regions of membrane order in MEF cells

In Chapter 2, I show that independent of conformational state or adhesion association, β1 integrins co-localize with both probes of conflicting phase preference at both one and 24-hour attachment at a magnitude of 10-15% enrichment. The primary interpretation of these results is that, in general, β1 integrins do not strongly associate regions of membrane order. This contradicts conclusions from past results that indicated adhesions were regions of higher membrane order than a canonical liquid-order marker, Cholera Toxin subunit B (CTxB) [100]. Another interpretation of these results is that adhesions are regions of more membrane content than the average cell membrane.

Analysis and segmentation of reconstructed images determined that integrins found within adhesions have a stronger preference for membrane order versus non-adhesion associated integrins. The trend is present in both early-stage attachment (one hour) and late-stage attachment (24-hour), with mature fibrillar adhesions exhibiting the strongest preference for membrane order. In both attachment stages, enrichment of a disorder-preferring peptide remains, albeit less than the order preferring. My results are consistent with previous results that demonstrate adhesions are regions of membrane order [12, 94, 100, 156], but I present evidence that β1 integrin containing fibrillar adhesions are more ordered than their earlier maturation-stage counterparts. However, since integrins found within adhesions associate with both membrane order and disorder preferring

probes I conclude integrins, independent of the conformational state, do not govern the membrane ordering found at adhesions.

I also determined there are advantages to computing the cross-correlation locally, i.e., within a fixed region around each adhesion. This approach eliminates long-scale averaging artifacts contributed by the directionality, size range, and subcellular location of the adhesion. This method results in a reduction of the enrichment of the disorder preferring probe from ~10% to that of a random-probe distribution inside and outside the adhesion. From this result, I can conclude that integrins prefer membrane order over disorder in mouse embyronic fibroblasts.

Finally, I extended the imaging and analysis scheme to examine integrin association with membrane order in an immortalized epithelial breast cancer cell line, MDA-MB-231. I found that adhesions are associated with membrane order and that the conformational state of integrins may be responsible for the membrane-ordering found in adhesions in epithelial cell lines.

In sum, the total β1 population integrins found within adhesions associated with membrane order over disorder in two varying cell lines. This is consistent with past reports on integrin-mediation adhesion sites being regions of membrane order. However, the presence of disordering preferring probes surrounding integrins indicates adhesions and integrins may not be as highly ordered as previously proposed. This conclusion is supported by the lack of anti-correlation between β1 integrins and disorder preferring markers. I conclude that independent of conformational state, β1 integrins alone do not govern the membrane-order environment found within adhesions.

4.3 Active β1 integrins do not exhibit a stronger preference for membrane order in MEFs

In Chapter 2, I examined the lipid landscape surrounding conformationally active β1 integrins in an immortalized epithelial line which demonstrated no short-length scale enrichment of a disorder favoring marker. This motivated the experiments to determine how β1 integrin activation state is associated with membrane order in fibroblasts. This lead to perhaps the most surprising result from this dissertation is that active conformation β1 integrins co-localize with both membrane order and disorder preferring probes. I conclude from these results that conformationally active β1 integrins are not the mediators of membrane order found in adhesions. The active conformation of integrins are also hypothesized to be actively signaling and responsible for clustering that forms adhesions [1-3, 145, 157]. I found that active conformation integrins do not always co-localize with phosphotyrosine, a downstream cell signaling marker. I conclude that to comment on adhesion or integrin activity, staining for active conformations alone is not enough.

4.4 Long-chain *n*-alcohols are capable of biasing integrin activation

In Chapter 3, I found the activation state of β1 integrins can be biased through incubation of two *n*-alcohols: 1-hexadecanol and 1-octanol. Both of these alcohols have previously shown to alter the physical properties of lipids [143, 144, 152] and are expected to change the size and lifetime of phase-like domains in the plasma membrane of intact cells. Results from my experiments revealed 1-hexadecanol increasing integrin engagement 19.1% ± 0.09 and 1-octanol decreasing integrin engagement by 22.9% ± 0.07 less than the control. Since I found that integrins alone do not have a strong association with protein markers membrane order, I conclude that the addition of the alcohols is likely affecting the inside-out activation network of integrins. One explanation is that the *n*-alcohols change the plasma membrane composition to increase or decrease levels of charged lipid species, specifically Phosphatidylinositol 4,5-bisphosphate (PIP2),

which has shown to be responsible for orienting integrin activating proteins talin and kindlin to the β1 integrin tails.

4.5 Notes on reagents and challenges that contribute to this work

One of the most significant challenges this research is access to antibodies that are both suitable for super-resolution imaging and functional in paraformaldehyde-glutaraldehyde-fixed cells. Moving to live-cell experiments would overcome this obstacle. Additionally, many of the commercial murine monoclonal antibodies targeting different integrin conformations use secondary antibodies of the same species, so doing multi-color super-resolution experiments is not possible. However, there are numerous well-characterized anti-human monoclonal antibodies available [24], so transitioning into a human cell line for future chemically fixed super-resolution experiments would be a better route versus staying with mouse fibroblasts

4.6 Lipid sensitive inside-out regulatory network of integrin activation provide context for results of this dissertation

The central result of this dissertation is that β1 integrin conformational state is not the main mediator of the membrane ordering characteristics found in adhesive sites in chemically fixed mouse fibroblasts. Additionally, the enrichment of liquid-disorder markers surrounding integrins demonstrates adhesions may not be as ordered as previously projected [100]. However, β1 integrin activation state can be biased through membrane perturbations as demonstrated by my *n*-alcohols studies and similar studies from other researchers [85-87]. This result calls for further experimentation exploring of the inside-out signaling regulatory network within cells that modulate integrin activation and avidity (i.e. "overall strength of cell adhesiveness" [158]) of β1 integrins. The cytoskeletal proteins, talin, kindlin, and the Focal Adhesion Kinase (FAK) are reported to be the proteins recruited early on to the β1 integrin tails and work together to activate

β1 integrins and/ or recruit proteins responsible for downstream signaling. Regulation of each of these proteins has in, at least in part, been shown to be sensitive to membrane composition or linked to liquid-order membrane domains which could contribute to β1-mediated adhesion sites to be associated with membrane domains [42, 159-162].

4.6.1 n-Alcohols are hypothesized to influence PIP2 levels and effect talin and kindlin recruitment for integrin activation

Talin and kindlins have shown to contribute to integrin activation by binding directly with the cytoplasmic domain the β1 integrin tails by disrupting a salt bridge that locks the legs of the α and β integrin subunits together. The lipid Phosphatidylinositol 4,5-bisphosphate (PIP2) orients talin and kindlin to the plasma membrane by interacting with a portion of their structurally similar FERM domains, for each of them to bind to the β1 integrin tails and contribute to integrin activation. PIP2-talin-kindlin interaction provides reasoning for why lipid composition regulates integrin activation. Studies have shown that cell exposure to shorter-chain alcohols reduce PIP2 levels and subsequently suppress PIP2-dependent processes [154, 155].The addition of alcohols could be changing global PIP2 levels in the plasma membrane, causing enhanced or reduced recruitment of talin and kindlin for subsequent integrin activation.

4.6.2 Proposed experiment to monitor the effect of PIP2 levels on inside-out activation of integrins

PIP2 levels can be monitored by antibody detection [163] or through expressible proteins with pleckstrin homology (PH) domains which bind to phosphoinositides [164-166]. The PH domain from the phospholipase C-δ1 (PLCδ-PH) specifically binds to PIP2 with high affinity and has a live-cell probe to localize PIP2 levels in cells [166]. These expressible PH domains are

particularly advantageous because they reversibly bind to PIP2 in the membrane, where others irreversibly bind to PIP2 and mask the functional charged residues.

I propose to monitor PIP2 levels using an expressible fluorescent variant of the PLCδ-PH probe before and after the addition of the *n*-alcohols, similar to the binding assay discussed in Chapter 3, section 3.4. I expect to see an increase of PIP2 after exposure to 1-hexadecanol and a decrease after exposure to 1-octanol. Partnered with this experiment, talin and/or kindlin recruitment will need to be monitored before and after the addition of alcohols. This will verify the importance of PIP2 levels and talin and/or kindlin to the membrane in intact cells. Both of these experiments will test the importance of PIP2s in integrin activation and demonstrate how membrane composition influences the first scaffolding proteins recruited to β1 tails.

4.6.3 Experiment testing n-alcohol effects on the function of the FAK-Src signaling complex

Liquid-ordered membrane domains have shown to have a role in the downstream signaling cascade that is initiated at activated adhesions or clustered integrins. In recent studies by Seong and colleagues, a cellular focal adhesion kinase/Src FRET biosensor was anchored to the plasma membrane with peptides that have shown to have conflicting order preference [101, 102]. One anchor isolated the biosensor to "Detergent-Resistant Membrane" (DRM) regions or liquid-order domains, and the other resided in disordered domains. These anchors are analogous the PM and TM peptides used in the two-color super-resolution data and results presented in Chapter 2 and 3. Seong and colleague's data indicate, while the anchored biosensors are distributed across the cell, FAK/Src activity was more active inside liquid-order domains. One interpretation of this data is that because the FAK/Src complex interacts with the active β1 tail that the integrin is dictating the membrane ordering characteristics. However, in the context of the conclusions presented in this

dissertation, I believe that the FAK/Src complex contributes the membrane ordering characteristics and not the integrin.

In this case, I propose to monitor the recruitment of active FAK before and after the addition of *n*-alcohols. This can be accomplished through antibody detection of phosphorylated-FAK (Y397), which is representative of the state of FAK that is no longer autoinhibited and can bind to Src. Results from this experiment will determine how the alcohol perturbations affect FAK/Src recruitment to the adhesion and will provide inside on how perturbing lipid composition directly affects adhesion signaling. Additionally, a functional FAK/Src signaling complex initiates many downstream pathways, but its phosphorylation of paxillin, an adaptor protein that resides in adhesions, is important for forming functional adhesions. Antibody staining of phospho-paxillin (Y118) could be another target in addition to phospho-FAK (Y397) to monitor how PIP2 levels affect the FAK/Src complex. I predict that 1-hexadecanol will increase PIP2 levels, increasing recruitment of FAK/Src to integrins, and increasing the amount of phospho-paxillin (Y118) at the adhesion.

4.6.4 Experiments to determine which adhesion components with strongest membrane ordering characteristics

Perhaps the most puzzling question that emerges from the results of this dissertation, if β1 integrins do not mediate the membrane order found in fibrillar adhesions, what does? I would first examine the cytoskeletal proteins or kinases found in adhesions that seem to have the strongest membrane association, e.g., talin, kindlin, FAK/Src complex with two color-super resolution localization microscopy experiments and analysis like those described in Chapters 2 and 3. It also a possibility that elevated PIP2 levels that are hypothesized to be in adhesions could also contribute to the membrane ordering characteristics found there [33, 38, 39]. If this is the case, a two-color

super-resolution experiment looking at the enrichment or depletion of membrane order marking probes could around the PLCδ-PH domain could determine if PIP2s contribute to the membrane order found in adhesions.

4.7 Concluding remarks

The work presented in this dissertation revealed that the conformational state of β1- integrins do not govern the membrane ordering found in adhesions, but their conformational state can be biased through biochemical membrane perturbations. This work also revealed that integrins and adhesion associated proteins have a complex relationship with their membrane environment, which needs further characterization. One of the challenges for the road ahead will be designing experiments that study integrins in their native membrane environment while sorting out the relationship between regulatory proteins that govern integrin activation. Consideration must also be given that the "inside out" and "outside in" modes of integrin activation, which are often discussed separately, likely happen nearly simultaneously in the cell's native environment and are mediated by the plasma membrane's composition.

References

1. Campbell, I.D. and M.J. Humphries, *Integrin Structure, Activation, and Interactions.* Cold Spring Harbor Perspectives in Biology, 2011. **3**(3): p. a004994.
2. Ginsberg, M.H., *Integrin activation.* BMB Rep, 2014. **47**(12): p. 655-9.
3. Shattil, S.J., C. Kim, and M.H. Ginsberg, *The final steps of integrin activation: the end game.* Nature Reviews Molecular Cell Biology, 2010. **11**(4): p. 288-300.
4. Shimaoka, M., J. Takagi, and T.A. Springer, *Conformational regulation of integrin structure and function.* Annu Rev Biophys Biomol Struct, 2002. **31**: p. 485-516.
5. Contributors, M. *Focal Adhesion Organization*. 2014 [cited 2014; Available from: http://mbinfo.mbi.nus.edu.sg/figure/1384243372096/.
6. Morgan, M.R., M.J. Humphries, and M.D. Bass, *Synergistic control of cell adhesion by integrins and syndecans.* Nat Rev Mol Cell Biol, 2007. **8**(12): p. 957-969.
7. Hynes, R.O., *Integrins.* Cell, 2002. **110**(6): p. 673-687.
8. Mouw, J.K., G. Ou, and V.M. Weaver, *Extracellular matrix assembly: a multiscale deconstruction.* Nat Rev Mol Cell Biol, 2014. **15**(12): p. 771-785.
9. Zaidel-Bar, R., et al., *Functional atlas of the integrin adhesome.* Nat Cell Biol, 2007. **9**(8): p. 858-867.
10. Winograd-Katz, S.E., et al., *The integrin adhesome: from genes and proteins to human disease.* Nat Rev Mol Cell Biol, 2014. **15**(4): p. 273-288.
11. Abercrombie, M. and G.A. Dunn, *Adhesions of fibroblasts to substratum during contact inhibition observed by interference reflection microscopy.* Experimental Cell Research, 1975. **92**(1): p. 57-62.
12. Albiges-Rizo, C., et al., *Actin machinery and mechanosensitivity in invadopodia, podosomes and focal adhesions.* Journal of Cell Science, 2009. **122**(17): p. 3037.
13. Vicente-Manzanares, M. and A.R. Horwitz, *Adhesion dynamics at a glance.* Journal of Cell Science, 2011. **124**(23): p. 3923.
14. Zamir, E., et al., *Dynamics and segregation of cell–matrix adhesions in cultured fibroblasts.* 2000. **2**: p. 191.
15. Zamir, E. and B. Geiger, *Molecular complexity and dynamics of cell-matrix adhesions.* Journal of Cell Science, 2001. **114**(20): p. 3583.
16. Watt, F.M., *Role of integrins in regulating epidermal adhesion, growth and differentiation.* Embo Journal, 2002. **21**(15): p. 3919-3926.
17. Fassler, R. and M. Meyer, *CONSEQUENCES OF LACK OF BETA-1 INTEGRIN GENE-EXPRESSION IN MICE.* Genes & Development, 1995. **9**(15): p. 1896-1908.

18. Martin, P., *Wound healing - Aiming for perfect skin regeneration.* Science, 1997. **276**(5309): p. 75-81.

19. Luo, B.H., C.V. Carman, and T.A. Springer, *Structural basis of integrin regulation and signaling.* Annu Rev Immunol, 2007. **25**: p. 619-47.

20. Cox, D., M. Brennan, and N. Moran, *Integrins as therapeutic targets: lessons and opportunities.* Nature Reviews Drug Discovery, 2010. **9**(10): p. 804-820.

21. Zhu, J., J. Zhu, and T.A. Springer, *Complete integrin headpiece opening in eight steps.* The Journal of Cell Biology, 2013. **201**(7): p. 1053-1068.

22. Springer, T.A. and M.L. Dustin, *Integrin inside-out signaling and the immunological synapse.* Current Opinion in Cell Biology, 2012. **24**(1): p. 107-115.

23. Li, J., et al., *Conformational equilibria and intrinsic affinities define integrin activation.* The EMBO Journal, 2017. **36**(5): p. 629-645.

24. Byron, A., et al., *Anti-integrin monoclonal antibodies.* Journal of Cell Science, 2009. **122**(22): p. 4009-4011.

25. Arnaout, M.A., S.L. Goodman, and J.P. Xiong, *Structure and mechanics of integrin-based cell adhesion.* Curr Opin Cell Biol, 2007. **19**(5): p. 495-507.

26. Xiong, J.P., et al., *Crystal structure of the extracellular segment of integrin alpha Vbeta3.* Science, 2001. **294**(5541): p. 339-45.

27. Zhang, K. and J.F. Chen, *The regulation of integrin function by divalent cations.* Cell Adhesion & Migration, 2012. **6**(1): p. 20-29.

28. Calderwood, D.A., I.D. Campbell, and D.R. Critchley, *Talins and kindlins: partners in integrin-mediated adhesion.* 2013. **14**: p. 503.

29. Orlowski, A., et al., *PIP2 and Talin Join Forces to Activate Integrin.* J Phys Chem B, 2015. **119**(38): p. 12381-9.

30. Arias-Salgado, E.G., et al., *Specification of the direction of adhesive signaling by the integrin beta cytoplasmic domain.* J Biol Chem, 2005. **280**(33): p. 29699-707.

31. McLaughlin, S., et al., *PIP(2) and proteins: interactions, organization, and information flow.* Annu Rev Biophys Biomol Struct, 2002. **31**: p. 151-75.

32. Xu, C., J. Watras, and L.M. Loew, *Kinetic analysis of receptor-activated phosphoinositide turnover.* J Cell Biol, 2003. **161**(4): p. 779-91.

33. Lupyan, D., et al., *A molecular dynamics investigation of lipid bilayer perturbation by PIP2.* Biophys J, 2010. **98**(2): p. 240-7.

34. Saltel, F., et al., *New PI(4,5)P2- and membrane proximal integrin-binding motifs in the talin head control beta3-integrin clustering.* J Cell Biol, 2009. **187**(5): p. 715-31.

35. Moore, D.T., et al., *Affinity of talin-1 for the beta3-integrin cytosolic domain is modulated by its phospholipid bilayer environment.* Proc Natl Acad Sci U S A, 2012. **109**(3): p. 793-8.

36. Ling, K., et al., *Type I gamma phosphatidylinositol phosphate kinase targets and regulates focal adhesions.* Nature, 2002. **420**(6911): p. 89-93.

37. Di Paolo, G., et al., *Recruitment and regulation of phosphatidylinositol phosphate kinase type 1 gamma by the FERM domain of talin.* Nature, 2002. **420**(6911): p. 85-9.

38. Taglieri, D.M., D.A. Delfin, and M.M. Monasky, *Cholesterol regulation of PIP(2): why cell type is so important.* Front Physiol, 2012. **3**: p. 492.

39. Pike, L.J. and J.M. Miller, *Cholesterol depletion delocalizes phosphatidylinositol bisphosphate and inhibits hormone-stimulated phosphatidylinositol turnover.* J Biol Chem, 1998. **273**(35): p. 22298-304.

40. Tomakidi, P., et al., *Focal adhesion kinase (FAK) perspectives in mechanobiology: implications for cell behaviour.* Cell Tissue Res, 2014. **357**(3): p. 515-26.

41. Hall, J.E., W. Fu, and M.D. Schaller, *Focal adhesion kinase: exploring Fak structure to gain insight into function.* Int Rev Cell Mol Biol, 2011. **288**: p. 185-225.

42. Mitra, S.K., D.A. Hanson, and D.D. Schlaepfer, *Focal adhesion kinase: in command and control of cell motility.* Nat Rev Mol Cell Biol, 2005. **6**(1): p. 56-68.

43. Parsons, J.T., *Focal adhesion kinase: the first ten years.* J Cell Sci, 2003. **116**(Pt 8): p. 1409-16.

44. Zhao, X. and J.L. Guan, *Focal adhesion kinase and its signaling pathways in cell migration and angiogenesis.* Adv Drug Deliv Rev, 2011. **63**(8): p. 610-5.

45. Ilic, D., et al., *Reduced cell motility and enhanced focal adhesion contact formation in cells from FAK-deficient mice.* Nature, 1995. **377**(6549): p. 539-44.

46. Cary, L.A., J.F. Chang, and J.L. Guan, *Stimulation of cell migration by overexpression of focal adhesion kinase and its association with Src and Fyn.* J Cell Sci, 1996. **109 (Pt 7)**: p. 1787-94.

47. Sieg, D.J., C.R. Hauck, and D.D. Schlaepfer, *Required role of focal adhesion kinase (FAK) for integrin-stimulated cell migration.* J Cell Sci, 1999. **112 (Pt 16)**: p. 2677-91.

48. Owen, J.D., et al., *Induced focal adhesion kinase (FAK) expression in FAK-null cells enhances cell spreading and migration requiring both auto- and activation loop phosphorylation sites and inhibits adhesion-dependent tyrosine phosphorylation of Pyk2.* Mol Cell Biol, 1999. **19**(7): p. 4806-18.

49. Hayashi, I., K. Vuori, and R.C. Liddington, *The focal adhesion targeting (FAT) region of focal adhesion kinase is a four-helix bundle that binds paxillin.* Nat Struct Biol, 2002. **9**(2): p. 101-6.

50. Frame, M.C., et al., *The FERM domain: organizing the structure and function of FAK.* Nat Rev Mol Cell Biol, 2010. **11**(11): p. 802-14.

51. Lietha, D., et al., *Structural basis for the autoinhibition of focal adhesion kinase.* Cell, 2007. **129**(6): p. 1177-87.

52. Bolos, V., et al., *The dual kinase complex FAK-Src as a promising therapeutic target in cancer.* Onco Targets Ther, 2010. **3**: p. 83-97.

53. Mitra, S.K. and D.D. Schlaepfer, *Integrin-regulated FAK-Src signaling in normal and cancer cells.* Curr Opin Cell Biol, 2006. **18**(5): p. 516-23.

54. Schaller, M.D., et al., *Focal adhesion kinase and paxillin bind to peptides mimicking beta integrin cytoplasmic domains.* J Cell Biol, 1995. **130**(5): p. 1181-7.

55. Huveneers, S. and E.H. Danen, *Adhesion signaling - crosstalk between integrins, Src and Rho.* J Cell Sci, 2009. **122**(Pt 8): p. 1059-69.

56. Westhoff, M.A., et al., *SRC-mediated phosphorylation of focal adhesion kinase couples actin and adhesion dynamics to survival signaling.* Mol Cell Biol, 2004. **24**(18): p. 8113-33.

57. Thomas, S.M. and J.S. Brugge, *Cellular functions regulated by Src family kinases.* Annu Rev Cell Dev Biol, 1997. **13**: p. 513-609.

58. Katz, B.Z., et al., *Targeting membrane-localized focal adhesion kinase to focal adhesions: roles of tyrosine phosphorylation and SRC family kinases.* J Biol Chem, 2003. **278**(31): p. 29115-20.

59. Arcaro, A., et al., *Critical role for lipid raft-associated Src kinases in activation of PI3K-Akt signalling.* Cell Signal, 2007. **19**(5): p. 1081-92.

60. Seong, J.Y., et al., *Detection of focal adhesion kinase activation at membrane microdomains by fluorescence resonance energy transfer.* Nature Communications, 2011. **2**: p. 9.

61. Singer, S.J. and G.L. Nicolson, *The Fluid Mosaic Model of the Structure of Cell Membranes.* Science, 1972. **175**(4023): p. 720.

62. Spector, A.A. and M.A. Yorek, *Membrane lipid composition and cellular function.* J Lipid Res, 1985. **26**(9): p. 1015-35.

63. Israelachvili, J.N., *Refinement of the fluid-mosaic model of membrane structure.* BBA - Biomembranes, 1977. **469**(2): p. 221-225.

64. Schuck, S. and K. Simons, *Polarized sorting in epithelial cells: raft clustering and the biogenesis of the apical membrane.* Journal of Cell Science, 2004. **117**(25): p. 5955.

65. Simons, K. and G. Van Meer, *Lipid sorting in epithelial cells.* Biochemistry, 1988. **27**(17): p. 6197-6202.

66. McNeil, P.L. and R.A. Steinhardt, *Loss, Restoration, and Maintenance of Plasma Membrane Integrity.* The Journal of Cell Biology, 1997. **137**(1): p. 1-4.

67. Pamplona, R., *Membrane phospholipids, lipoxidative damage and molecular integrity: A causal role in aging and longevity.* Biochimica et Biophysica Acta (BBA) - Bioenergetics, 2008. **1777**(10): p. 1249-1262.

68. Hannun, Y.A. and L.M. Obeid, *Principles of bioactive lipid signalling: lessons from sphingolipids.* 2008. **9**: p. 139.

69. Wymann, M.P. and R. Schneiter, *Lipid signalling in disease.* 2008. **9**: p. 162.

70. Shevchenko, A. and K. Simons, *Lipidomics: coming to grips with lipid diversity.* Nature Reviews Molecular Cell Biology, 2010. **11**(8): p. 593-598.

71. Janiak, M.J., D.M. Small, and G.G. Shipley, *Temperature and compositional dependence of the structure of hydrated dimyristoyl lecithin.* J Biol Chem, 1979. **254**(13): p. 6068-78.

72. Ipsen, J.H., O.G. Mouritsen, and M.J. Zuckermann, *Theory of thermal anomalies in the specific heat of lipid bilayers containing cholesterol.* Biophys J, 1989. **56**(4): p. 661-7.

73. Veatch, S.L. and S.L. Keller, *Seeing spots: complex phase behavior in simple membranes.* Biochim Biophys Acta, 2005. **1746**(3): p. 172-85.

74. van Meer, G., D.R. Voelker, and G.W. Feigenson, *Membrane lipids: where they are and how they behave.* Nat Rev Mol Cell Biol, 2008. **9**(2): p. 112-124.

75. Lewis, R.N. and R.N. McElhaney, *Membrane lipid phase transitions and phase organization studied by Fourier transform infrared spectroscopy.* Biochim Biophys Acta, 2013. **1828**(10): p. 2347-58.

76. Elson, E.L., et al., *Phase separation in biological membranes: integration of theory and experiment.* Annu Rev Biophys, 2010. **39**: p. 207-26.

77. Heberle, F.A. and G.W. Feigenson, *Phase separation in lipid membranes.* Cold Spring Harb Perspect Biol, 2011. **3**(4).

78. Yellin, N. and I.W. Levin, *Hydrocarbon trans-gauche isomerization in phospholipid bilayer gel assemblies.* Biochemistry, 1977. **16**(4): p. 642-7.

79. Simons, K. and W.L.C. Vaz, *Model Systems, Lipid Rafts, and Cell Membranes.* Annual Review of Biophysics and Biomolecular Structure, 2004. **33**(1): p. 269-295.

80. Almeida, P.F., W.L. Vaz, and T.E. Thompson, *Percolation and diffusion in three-component lipid bilayers: effect of cholesterol on an equimolar mixture of two phosphatidylcholines.* Biophys J, 1993. **64**(2): p. 399-412.

81. Filippov, A., G. Oradd, and G. Lindblom, *The effect of cholesterol on the lateral diffusion of phospholipids in oriented bilayers.* Biophys J, 2003. **84**(5): p. 3079-86.

82. Ipsen, J.H., et al., *Phase equilibria in the phosphatidylcholine-cholesterol system.* Biochim Biophys Acta, 1987. **905**(1): p. 162-72.

83. Gally, H.U., A. Seelig, and J. Seelig, *Cholesterol-induced rod-like motion of fatty acyl chains in lipid bilayers a deuterium magnetic resonance study.* Hoppe Seylers Z Physiol Chem, 1976. **357**(10): p. 1447-50.

84. Gopalakrishna, P., et al., *Modulation of alpha5beta1 integrin functions by the phospholipid and cholesterol contents of cell membranes.* J Cell Biochem, 2000. **77**(4): p. 517-28.

85. Ramprasad, O.G., et al., *Changes in cholesterol levels in the plasma membrane modulate cell signaling and regulate cell adhesion and migration on fibronectin.* Cell Motility and the Cytoskeleton, 2007. **64**(3): p. 199-216.

86. Dibya, D., N. Arora, and E.A. Smith, *Noninvasive measurements of integrin microclustering under altered membrane cholesterol levels.* Biophys J, 2010. **99**(3): p. 853-61.

87. Green, J.M., et al., *Role of Cholesterol in Formation and Function of a Signaling Complex Involving αvβ3, Integrin-Associated Protein (Cd47), and Heterotrimeric G Proteins.* The Journal of Cell Biology, 1999. **146**(3): p. 673-682.

88. Eich, C., et al., *Changes in membrane sphingolipid composition modulate dynamics and adhesion of integrin nanoclusters.* Scientific reports, 2016. **6**: p. 20693.

89. Sharma, D.K., et al., *The glycosphingolipid, lactosylceramide, regulates beta1-integrin clustering and endocytosis.* Cancer Res, 2005. **65**(18): p. 8233-41.

90. Nagasato, A.I., et al., *The distribution of vinculin to lipid rafts plays an important role in sensing stiffness of extracellular matrix.* Bioscience Biotechnology and Biochemistry, 2017. **81**(6): p. 1136-1147.

91. Grove, L.M., et al., *Urokinase-type Plasminogen Activator Receptor (uPAR) Ligation Induces a Raft-localized Integrin Signaling Switch That Mediates the Hypermotile Phenotype of Fibrotic Fibroblasts.* Journal of Biological Chemistry, 2014. **289**(18): p. 12791-12804.

92. Wang, R.F., et al., *Lipid rafts control human melanoma cell migration by regulating focal adhesion disassembly.* Biochimica Et Biophysica Acta-Molecular Cell Research, 2013. **1833**(12): p. 3195-3205.

93. Ouchani, F., et al., *Targeting focal adhesion assembly by ethoxyfagaronine prevents lymphoblastic cell adhesion to fibronectin.* Analytical Cellular Pathology, 2012. **35**(4): p. 267-284.

94. Porter, J.C. and N. Hogg, *Integrins take partners: cross-talk between integrins and other membrane receptors.* Trends in Cell Biology, 1998. **8**(10): p. 390-396.

95. van Zanten, T.S., et al., *Hotspots of GPI-anchored proteins and integrin nanoclusters function as nucleation sites for cell adhesion.* Proceedings of the National Academy of Sciences of the United States of America, 2009. **106**(44): p. 18557-18562.

96. del Pozo, M.A., et al., *Integrins regulate Rac targeting by internalization of membrane domains.* Science, 2004. **303**(5659): p. 839-842.

97. Ge, Y., et al., *Ligand Binding Alters Dimerization and Sequestering of Urokinase Receptors in Raft-Mimicking Lipid Mixtures.* Biophysical Journal, 2014. **107**(9): p. 2101-2111.

98. Hussain, Noor F., et al., *Bilayer Asymmetry Influences Integrin Sequestering in Raft-Mimicking Lipid Mixtures.* Biophysical Journal, 2013. **104**(10): p. 2212-2221.

99. Siegel, A.P., et al., *Native Ligands Change Integrin Sequestering but Not Oligomerization in Raft-Mimicking Lipid Mixtures.* Biophysical Journal, 2011. **101**(7): p. 1642-1650.

100. Gaus, K., et al., *Integrin-mediated adhesion regulates membrane order.* Journal of Cell Biology, 2006. **174**(5): p. 725-734.

101. Seong, J., S. Lu, and Y. Wang, *Live Cell Imaging of Src/FAK Signaling by FRET.* Cell Mol Bioeng, 2011. **2**(4): p. 138-147.

102. Seong, J., et al., *Detection of focal adhesion kinase activation at membrane microdomains by fluorescence resonance energy transfer.* Nature Communications, 2011. **2**: p. 406.

103. Rust, M.J., M. Bates, and X. Zhuang, *Sub-diffraction-limit imaging by stochastic optical reconstruction microscopy (STORM).* Nature Methods, 2006. **3**: p. 793.

104. Heilemann, M., et al., *Carbocyanine Dyes as Efficient Reversible Single-Molecule Optical Switch.* Journal of the American Chemical Society, 2005. **127**(11): p. 3801-3806.

105. Hess, S.T., T.P.K. Girirajan, and M.D. Mason, *Ultra-High Resolution Imaging by Fluorescence Photoactivation Localization Microscopy.* Biophysical Journal, 2006. **91**(11): p. 4258-4272.

106. Betzig, E., et al., *Imaging Intracellular Fluorescent Proteins at Nanometer Resolution.* Science, 2006. **313**(5793): p. 1642.

107. Kanchanawong, P., et al., *Nanoscale architecture of integrin-based cell adhesions.* Nature, 2010. **468**(7323): p. 580-4.

108. Rossier, O., et al., *Integrins β1 and β3 exhibit distinct dynamic nanoscale organizations inside focal adhesions.* Nature Cell Biology, 2012. **14**: p. 1057.

109. Morimatsu, M., et al., *Visualizing the interior architecture of focal adhesions with high-resolution traction maps.* Nano Lett, 2015. **15**(4): p. 2220-8.

110. Kato, H., et al., *The Primacy of β1 Integrin Activation in the Metastatic Cascade.* PLOS ONE, 2012. **7**(10): p. e46576.

111. Simons, K. and E. Ikonen, *Functional rafts in cell membranes.* Nature, 1997. **387**(6633): p. 569-572.

112. Stone, M.B., et al., *Protein sorting by lipid phase-like domains supports emergent signaling function in B lymphocyte plasma membranes.* Elife, 2017. **6**.

113. Stone, M.B., S.A. Shelby, and S.L. Veatch, *Super-Resolution Microscopy: Shedding Light on the Cellular Plasma Membrane.* Chemical Reviews, 2017. **117**(11): p. 7457-7477.

114. Cheng, P.C., et al., *A role for lipid rafts in B cell antigen receptor signaling and antigen targeting.* J Exp Med, 1999. **190**(11): p. 1549-60.

115. Petrie, R.J., et al., *Transient translocation of the B cell receptor and Src homology 2 domain-containing inositol phosphatase to lipid rafts: evidence toward a role in calcium regulation.* J Immunol, 2000. **165**(3): p. 1220-7.

116. Guo, B., et al., *Engagement of the human pre-B cell receptor generates a lipid raft-dependent calcium signaling complex.* Immunity, 2000. **13**(2): p. 243-53.

117. Weintraub, B.C., et al., *Entry of B cell receptor into signaling domains is inhibited in tolerant B cells.* J Exp Med, 2000. **191**(8): p. 1443-8.

118. Kabouridis, P.S., *Lipid rafts in T cell receptor signalling (Review).* Molecular membrane biology, 2006. **23**(1): p. 49-57.

119. Jury, E.C., F. Flores-Borja, and P.S. Kabouridis, *Lipid rafts in T cell signalling and disease.* Seminars in Cell & Developmental Biology, 2007. **18**(5-3): p. 608-615.

120. Wu, W., X. Shi, and C. Xu, *Regulation of T cell signalling by membrane lipids.* Nature Reviews Immunology, 2016. **16**: p. 690.

121. Pyenta, P.S., D. Holowka, and B. Baird, *Cross-Correlation Analysis of Inner-Leaflet-Anchored Green Fluorescent Protein Co-Redistributed with IgE Receptors and Outer Leaflet Lipid Raft Components.* Biophysical Journal, 2001. **80**(5): p. 2120-2132.

122. Levental, I., et al., *Palmitoylation regulates raft affinity for the majority of integral raft proteins.* Proceedings of the National Academy of Sciences, 2010. **107**(51): p. 22050-22054.

123. Sander, J., et al., *Density-based clustering in spatial databases: The algorithm GDBSCAN and its applications.* Data Mining and Knowledge Discovery, 1998. **2**(2): p. 169-194.

124. Xu, X.W., et al., *A distribution-based clustering algorithm for mining in large spatial databases*, in *14th International Conference on Data Engineering, Proceedings*. 1998, Ieee Computer Soc: Los Alamitos. p. 324-331.

125. Hood, J.D. and D.A. Cheresh, *Role of integrins in cell invasion and migration.* Nature Reviews Cancer, 2002. **2**(2): p. 91-+.

126. Varner, J.A. and D.A. Cheresh, *Integrins and cancer.* Current Opinion in Cell Biology, 1996. **8**(5): p. 724-730.

127. He, M., S. Guo, and Z. Li, *In situ characterizing membrane lipid phenotype of breast cancer cells using mass spectrometry profiling.* Scientific Reports, 2015. **5**: p. 11298.

128. Guo, W.J. and F.G. Giancotti, *Integrin signalling during tumour progression.* Nature Reviews Molecular Cell Biology, 2004. **5**(10): p. 816-826.

129. Clyman, R.I., F. Mauray, and R.H. Kramer, *Beta 1 and beta 3 integrins have different roles in the adhesion and migration of vascular smooth muscle cells on extracellular matrix.* Exp Cell Res, 1992. **200**(2): p. 272-84.

130. Veatch, S.L., et al., *Correlation Functions Quantify Super-Resolution Images and Estimate Apparent Clustering Due to Over-Counting.* PLOS ONE, 2012. **7**(2): p. e31457.

131. Luo, B.H. and T.A. Springer, *Integrin structures and conformational signaling.* Curr Opin Cell Biol, 2006. **18**(5): p. 579-86.

132. Askari, J.A., et al., *Focal adhesions are sites of integrin extension.* J Cell Biol, 2010. **188**(6): p. 891-903.

133. Frelinger, A.L., 3rd, et al., *Selective inhibition of integrin function by antibodies specific for ligand-occupied receptor conformers.* J Biol Chem, 1990. **265**(11): p. 6346-52.

134. Mould, A.P., *Getting integrins into shape: recent insights into how integrin activity is regulated by conformational changes.* J Cell Sci, 1996. **109 (Pt 11)**: p. 2613-8.

135. Xiong, J.P., et al., *Crystal structure of the extracellular segment of integrin alpha Vbeta3 in complex with an Arg-Gly-Asp ligand.* Science, 2002. **296**(5565): p. 151-5.

136. Xiao, T., et al., *Structural basis for allostery in integrins and binding to fibrinogen-mimetic therapeutics.* Nature, 2004. **432**(7013): p. 59-67.

137. Beglova, N., et al., *Cysteine-rich module structure reveals a fulcrum for integrin rearrangement upon activation.* Nat Struct Biol, 2002. **9**(4): p. 282-7.

138. Takagi, J., et al., *Global conformational rearrangements in integrin extracellular domains in outside-in and inside-out signaling.* Cell, 2002. **110**(5): p. 599-11.

139. Nishida, N., et al., *Activation of leukocyte beta2 integrins by conversion from bent to extended conformations.* Immunity, 2006. **25**(4): p. 583-94.

140. Askari, J.A., et al., *Linking integrin conformation to function.* Journal of Cell Science, 2009. **122**(2): p. 165-170.

141. Chigaev, A. and L.A. Sklar, *Overview: assays for studying integrin-dependent cell adhesion.* Methods in molecular biology (Clifton, N.J.), 2012. **757**: p. 3-14.

142. Yan, B. and J.W. Smith, *Mechanism of integrin activation by disulfide bond reduction.* Biochemistry, 2001. **40**(30): p. 8861-7.

143. Gray, E., et al., *Liquid General Anesthetics Lower Critical Temperatures in Plasma Membrane Vesicles.* Biophysical Journal, 2013. **105**(12): p. 2751-2759.

144. Machta, B.B., et al., *Conditions that Stabilize Membrane Domains Also Antagonize n-Alcohol Anesthesia.* Biophys J, 2016. **111**(3): p. 537-545.

145. Calderwood, D.A., *Integrin activation.* Journal of Cell Science, 2004. **117**(5): p. 657.

146. Gahmberg, C.G., et al., *Regulation of integrin activity and signalling.* Biochim Biophys Acta, 2009. **1790**(6): p. 431-44.

147. Chen, S.Y., et al., *The membrane disordering effect of ethanol on neural crest cells in vitro and the protective role of GM1 ganglioside.* Alcohol, 1996. **13**(6): p. 589-95.

148. Rifici, S., et al., *Lipid diffusion in alcoholic environment.* J Phys Chem B, 2014. **118**(31): p. 9349-55.

149. Dickey, A.N. and R. Faller, *How alcohol chain-length and concentration modulate hydrogen bond formation in a lipid bilayer.* Biophys J, 2007. **92**(7): p. 2366-76.

150. Pang, K.Y., T.L. Chang, and K.W. Miller, *On the coupling between anesthetic induced membrane fluidization and cation permeability in lipid vesicles.* Mol Pharmacol, 1979. **15**(3): p. 729-38.

151. Ly, H.V. and M.L. Longo, *The influence of short-chain alcohols on interfacial tension, mechanical properties, area/molecule, and permeability of fluid lipid bilayers.* Biophys J, 2004. **87**(2): p. 1013-33.

152. Desai, R., *RBL-2H3 Proliferation is Modulated by Treatments That Shift Transition Temperature in Isolated Plasma Mebrane Vesicles*, in *Biophysics*. 2017, University of Michigan: Ann Arbor, MI. p. 33.

153. Humphries, M.J., et al., *Integrin structure: heady advances in ligand binding, but activation still makes the knees wobble.* Trends in Biochemical Sciences, 2003. **28**(6): p. 313-320.

154. Tong, W. and G.Y. Sun, *Effects of Ethanol on Phosphorylation of Lipids in Rat Synaptic Plasma Membranes.* Alcoholism: Clinical and Experimental Research, 1996. **20**(8): p. 1335-1339.

155. Hoffman, P.L., et al., *Acute and chronic effects of ethanol on receptor-mediated phosphatidylinositol 4,5-bisphosphate breakdown in mouse brain.* Molecular Pharmacology, 1986. **30**(1): p. 13.

156. Leitinger, B. and N. Hogg, *The involvement of lipid rafts in the regulation of integrin function.* Journal of Cell Science, 2002. **115**(5): p. 963.

157. Iwamoto, D.V. and D.A. Calderwood, *Regulation of integrin-mediated adhesions.* Current Opinion in Cell Biology, 2015. **36**(Supplement C): p. 41-47.

158. Carman, C.V. and T.A. Springer, *Integrin avidity regulation: are changes in affinity and conformation underemphasized?* Current Opinion in Cell Biology, 2003. **15**(5): p. 547-556.

159. Wang, R., et al., *Lipid raft regulates the initial spreading of melanoma A375 cells by modulating β1 integrin clustering.* The International Journal of Biochemistry & Cell Biology, 2013. **45**(8): p. 1679-1689.

160. Viola, A. and N. Gupta, *Tether and trap: regulation of membrane-raft dynamics by actin binding proteins.* Nature Reviews Immunology, 2007. **7**: p. 995.

161. Pande, G., *The role of membrane lipids in regulation of integrin functions.* Current Opinion in Cell Biology, 2000. **12**(5): p. 569-574.

162. Wickström, S.A. and R. Fässler, *Regulation of membrane traffic by integrin signaling.* Trends in Cell Biology, 2011. **21**(5): p. 266-273.

163. van den Bogaart, G., et al., *Membrane protein sequestering by ionic protein-lipid interactions.* Nature, 2011. **479**(7374): p. 552-5.

164. James, D.J., et al., *Phosphatidylinositol 4,5-bisphosphate regulates SNARE-dependent membrane fusion.* J Cell Biol, 2008. **182**(2): p. 355-66.

165. Griesbeck, O., et al., *Reducing the environmental sensitivity of yellow fluorescent protein. Mechanism and applications.* J Biol Chem, 2001. **276**(31): p. 29188-94.

166. Szentpetery, Z., et al., *Live cell imaging with protein domains capable of recognizing phosphatidylinositol 4, 5-bisphosphate; a comparative study.* BMC cell biology, 2009. **10**(1): p. 67.